CATEGORY B

ELECTRONIC COMPUTER PROGRAM ABSTRACT

TITLE OF PROGRAM	PROGRAM NO.
Analysis of One Dimensional Consolidation - FD31 (I0011)	741-F3-R0106

PREPARING AGENCY U. S. Army Engineer Waterways Experiment Station, Automatic Data Processing Center, P. O. Box 631, Vicksburg, MS 39180

AUTHOR(S)	DATE PROGRAM COMPLETED	STATUS OF PROGRAM	
		PHASE	STAGE
Dr. Roy Olson, Univ. of Texas Modified by: Reed Mosher, WES	1980		

A. PURPOSE OF PROGRAM

FD31 is a computer program which computes the settlements and rates of settlement in a multi-layered cohesive soil profile.

B. PROGRAM SPECIFICATIONS

C. METHODS

The settlements and rates of settlement are computed by the use of finite difference methods applied by Terzaghi's one-dimensional consolidation theory.

D. EQUIPMENT DETAILS

Standard equipment: Honeywell 600, 6600-Series

E. INPUT-OUTPUT

Input is read into program in free field from a data file interactively from the terminal.

Output is printed to the terminal and/or the outfile.

F. ADDITIONAL REMARKS

This program is included in the CORPS system. Complete documentation is available from the Engineering Computer Programs Library (ECPL), WES.

```
C*************************************************************************
C*                                                                       *
C*                          CONDITIONS OF USE                            *
C*                                                                       *
C*************************************************************************
C*                                                                       *
C*      THE FOLLOWING CONDITIONS REGULATE THE USE OF COMPUTER PROGRAMS   *
C*      DEVELOPED BY THE CORPS OF ENGINEERS, DEPARTMENT OF THE ARMY*     *
C*                                                                       *
C*      1.  THE COMPUTER PROGRAMS ARE FURNISHED BY THE GOVERNMENT AND    *
C*      MAKES NO WARRANTIES, EXPRESS OR IMPLIED, CONCERNING THE          *
C*      ACCURACY, COMPLETENESS, RELIABILITY, USABILITY, OR SUITABILITY   *
C*      FOR ANY PARTICULAR PURPOSE OF THE INFORMATION OR DATA CONTAINED  *
C*      IN THE PROGRAMS, OR FURNISHED IN CONNECTION THEREWITH, AND THE   *
C*      UNITED STATES SHALL BE UNDER NO LIABILITY WHATSOEVER TO ANY      *
C*      SUCH INDIVIDUAL OR GROUP ENTITY BY REASON OF ANY USE MADE        *
C*      THEREOF.                                                         *
C*                                                                       *
C*      2.  THE PROGRAMS BELONG TO THE FEDERAL GOVERNMENT.  THEREFORE,   *
C*      THE RECIPIENT AGREES NOT TO ASSERT ANY PROPRIETARY RIGHTS        *
C*      PROGRAMS AND ALL DOCUMENTS RELATED THERETO, INCLUDING ALL        *
C*      COPIES AND VERSIONS IN POSSESSION THEREOF, WILL BE DISCONTINUED  *
C*      FROM USE OR DESTROYED UPON REQUEST BY THE GOVERNMENT.            *
C*                                                                       *
C*      3.  THE PROGRAMS ARE TO BE USED ONLY IN THE PUBLIC INTEREST      *
C*      AND/OR THE ADVANCEMENT OF SCIENCE AND WILL NOT BE USED BY THE    *
C*      RECIPIENT TO GAIN UNFAIR ADVANTAGE OVER ANY CLIENT OR            *
C*      COMPETITOR.  WHEREAS THE RECIPIENT MAY CHARGE CLIENTS FOR THE    *
C*      ORDINARY COSTS OF APPLYING THESE PROGRAMS, THE RECIPIENT AGREES  *
C*      NOT TO LEVY A CHARGE, ROYALTY OR PROPRIETARY USAGE FEE UPON ANY  *
C*      CLIENT FOR THE DEVELOPMENT OR USE OF ANY PROGRAM RECEIVED, OR    *
C*      FOR ANY MODIFICATION OF SUCH PROGRAM BY THE RECIPIENT.  ONLY     *
C*      MINOR OR TEMPORARY MODIFICATIONS WILL BE MADE TO THE PROGRAMS    *
C*      (E.G., NECESSARY CORRECTIONS OR CHANGES IN THE FORMAT OF INPUT   *
C*      OR OUTPUT) WITHOUT WRITTEN APPROVAL FROM THE GOVERNMENT.  THE    *
C*      PROGRAMS WILL NOT BE FURNISHED BY THE RECIPIENT TO ANY THIRD     *
C*      PARTY UNDER ANY CIRCUMSTANCE.  HOWEVER, INFORMATION ON THE       *
C*      SOURCE OF THE PROGRAMS WILL BE FURNISHED TO ANYONE REQUESTING    *
C*      SUCH INFORMATION.                                                *
C*                                                                       *
C*      4.  ALL DOCUMENTS AND REPORTS CONVEYING INFORMATION OBTAINED AS  *
C*      A RESULT OF THE USE OF THE PROGRAM(S) BY THE RECIPIENT WILL      *
C*      ACKNOWLEDGE THE CORPS OF ENGINEERS, DEPARTMENT OF THE ARMY, AS   *
C*      THE ORIGIN OF THE PROGRAM(S) AND FOR ANY ASSISTANCE RECEIVED IN  *
C*      THEIR APPLICATION.                                               *
C*                                                                       *
C*************************************************************************
```

ANALYSIS OF

ONE DIMENSIONAL CONSOLIDATION PROBLEMS

WITH EMPHASIS ON

PROGRAM FD31

This report is intended to serve as a rationale for the use of finite difference methods of analysis of one dimensional consolidation problems and as a user's manual for one program, FD31. As the name implies, FD31 is one program in an evolutionary sequence of programs of increasing sophistication. It continues to evolve as deficiencies are found in existing versions. We are interested in being kept informed of any problems that develop in use of this program.

Roy E. Olson
4302 Far West Blvd.
Austin, Texas 78731

Phone: (512) 345-8996

TABLE OF CONTENTS

LIST OF TABLES

LIST OF FIGURES

CHAPTER 1

INTRODUCTION

The term consolidation is used to describe a process whereby fluid is forced out of the void spaces in a soil to allow the soil to decrease in volume. The term is also used in a more general way to include swelling as well as compression. The term one-dimensional consolidation refers to a consolidation process in which both fluid flow and deformation occur along a single axis. In field problems this axis is vertical. Because soils are not infinitely permeable, time is needed for escape of pore fluid; thus, consolidation is a time-dependent process.

One-dimensional consolidation typically occurs under the central regions of structures that are wide compared with the depth of compressible soil beneath the structure. Typical structures include wide fills, tanks, and raft foundations. One-dimensional conditions do not occur beneath typical spread footings but the assumption of one-dimensional compressibility is typically made to simplify analysis. The same assumption is typically made for highway embankments and numerous other structures. Sometimes a one-dimensional analysis is performed and then appropriate adjustments are made in the results to account for effects of deformation or flow in other directions; the adjustment factors may come from improved theories or from previous experience.

Nearly all practical analyses are performed using what we will term the "classical method." When this method is applied, the total compression is first calculated using a suitable one-dimensional stress-strain curve for the soil, and then the time rate of compression is calculated using Terzaghi's theory. This theory, and a number of simple extensions of it, will be reviewed in the next two sections.

That part of consolidation that is described by Terzaghi's theory is commonly termed primary consolidation. Effects not described by Terzaghi's theory are often referred to as secondary effects. The terms secondary consolidation, secondary compression, secular time effects,

and creep, are often used to describe these effects as well. A few of the theories involving secondary consolidation have been developed but, to our knowledge, none of these theories have been used for the analysis of practical projects nor have they even found their way into commonly used text books in geotechnical engineering.

Based on the discussions of the theories of consolidation, and the review of laboratory and field data, it will become apparent that the most useful method of analysis at the present time is to apply a basic Terzaghi model of consolidation but to generalize most of his simplifying assumptions to match field conditions, and to use a numerical method of analysis to solve the resulting equations. A sophisticated finite-difference method of analysis will be presented and a user's manual will be included for the computer program FD31.

The remaining chapters of this report are organized as follows:

- Fundamentals of Terzaghi's Theory
- Extensions to Terzaghi's Theory
- Laboratory Observations
- Field Observations
- Finite Difference Method of Analysis
- Computer Program FD31
- Concluding Remarks
- References

There are five appendices to this report:

A. List of Variables in Program FD31
B. Flow Diagrams for Program FD31
C. Listing of Program FD31
D. User's Guide for Program FD31
E. Examples of Input and Output for Program FD31.

CHAPTER 2

FUNDAMENTALS OF TERZAGHI'S THEORY

Because Terzaghi's theory is discussed in essentially all textbooks in soil mechanics, it will not be discussed in detail in this report. The equations, and the assumptions upon which they are based, will be presented as a basis for the discussion to follow.

Terzaghi's theory of consolidation is based on the following assumptions (Terzaghi, 1923, 1925; Terzaghi and Frölich, 1936):

1. The soil is a two-phase system composed of solid mineral matter and pore water. The water may contain dissolved gas but no free gas bubbles.
2. The soil is homogeneous.
3. The soil solids are incompressible compared with the water in the voids.
4. The pore water is incompressible compared with the soil structure.
5. Darcy's law is valid.
6. Changes in volume of the soil are so small during consolidation that constant average properties and dimensions may be used in the analysis.
7. The deformation is one dimensional.
8. The flow of pore water is one dimensional and along the same axis as the deformation.
9. The soil structure offers no time-dependent resistance to volume change.
10. The loading is instantaneous.

Based on these assumptions Terzaghi derived the following governing differential equation:

$$\frac{\partial \bar{u}}{\partial t} = c_v \frac{\partial^2 \bar{u}}{\partial z^2} \qquad (2.1)$$

where $\bar{u}$ is the excess pore water pressure, t is time, z is depth, and c_v is the coefficient of consolidation.

The excess pore water pressure is the excess above the static pore water pressure:

$$\bar{u} = u - u_s \quad \ldots\ldots\ldots\ldots\ldots\ldots \quad (2.2)$$

where u is the total pore water pressure and u_s is the static value, i.e., the value corresponding to final equilibrium without any flow.

The coefficient of consolidation, c_v is defined as:

$$c_v = \frac{k_v(1+e)}{a_v \gamma_w} \quad \ldots\ldots\ldots\ldots\ldots\ldots \quad (2.3)$$

where k_v is the coefficient of permeability, e is void ratio, a_v is the coefficient of compressibility, and γ_w is the unit weight of water. The coefficient of compressibility is defined as:

$$a_v = -\frac{de}{d\bar{\sigma}} \quad \ldots\ldots\ldots\ldots\ldots\ldots \quad (2.4)$$

where $\bar{\sigma}$ is the effective stress.

For a compressible layer of thickness 2H, with freely draining upper and lower boundaries, and a constant initial excess pore water pressure $\bar{u}_o$, the solution of Eq. 2.1 is:

$$\bar{u} = \sum_{m=0}^{\infty} \frac{2\bar{u}_o}{M} \sin(Mz/H)\exp(-M^2T) \quad \ldots\ldots \quad (2.5)$$

where M is defined as:

$$M = \tfrac{1}{2}\pi(2m+1) \quad \ldots\ldots\ldots\ldots\ldots\ldots \quad (2.6)$$

and T is <u>time factor</u> defined as:

$$T = c_v t/H^2 \quad \ldots\ldots\ldots\ldots\ldots\ldots \quad (2.7)$$

It is convenient to define the <u>average degree of consolidation</u>, U, as:

$$U = \frac{\int_0^{2H} \bar{u}_o dz - \int_0^{2H} \bar{u} dz}{\int_0^{2H} \bar{u}_o dz} \quad \ldots\ldots\ldots\ldots\ldots\ldots \quad (2.8)$$

CHAPTER 3

EXTENSIONS OF TERZAGHI'S THEORY

Terzaghi's theory can easily be extended to include cases involving non-uniform initial excess pore water pressures, time dependent loading, and partially draining boundaries. With more effort the theory can be extended to include layered systems, large strains, non-Darcy water flow, and other effects. The relatively simple extensions of Terzaghi's theory have found limited use by practicing engineers but the more complicated solutions seem to be of use mainly to researchers.

In this section a series of closed-form extensions of Terzaghi's theory will be presented both because of their direct use in engineering practice and because they will subsequently be used to check the accuracy of numerical solutions.

Non-Uniform Initial Excess Pore Water Pressures

When the initial excess pore water pressure is a function of depth, i.e., $\bar{u}_o = f(z)$, the solution for excess pore water pressure is obtained using:

$$u = \sum_{n=1}^{\infty} \{(1/H)\int_0^{2H} f(z)\sin(n\pi z/2H)dz\}\sin(n\pi z/2H)\exp(-n^2\pi^2 T/4) \quad . \quad . \quad (3.1)$$

A number of solutions will be found in Terzaghi and Fröhlich (1936). The only solutions of apparent practical significance are those for a triangular or sinusoidal variation in initial excess pore pressure.

For brevity, the term stress surface will be used to indicate the initial distribution of excess pore water pressure.

Triangular stress surface. A triangular stress surface can be generated in the field by suddenly dewatering a lower sand layer, by the destruction of an artesian condition, or by the sudden rising of the water surface in an upper sand while maintaining the same water level in a lower sand (Fig. 3.1). It is convenient to define the z axis as being measured

Substitution of Eq. 2.5 into Eq. 2.8 and integration yields:

$$U = 1 - \sum_{m=0}^{\infty} (2/M^2) \exp(-M^2 T) \quad \ldots\ldots\ldots\ldots \quad (2.9)$$

For the case of a constant coefficient of compressibility it may be shown that the settlement (S) due to compression of the layer under consideration, is related to the ultimate settlement (S_u) by:

$$S = U S_u \quad \ldots\ldots\ldots\ldots\ldots\ldots \quad (2.10)$$

In the classical method of analysis to obtain a time-settlement curve, the ultimate settlement is calculated first, using techniques presented in standard soil mechanics text books. Then the relationship between T and U is obtained (Eq. 2.9) from published solutions. Finally, time factors are converted to real time using Eq. 2.7 and degrees of consolidation to settlement using Eq. 2.10.

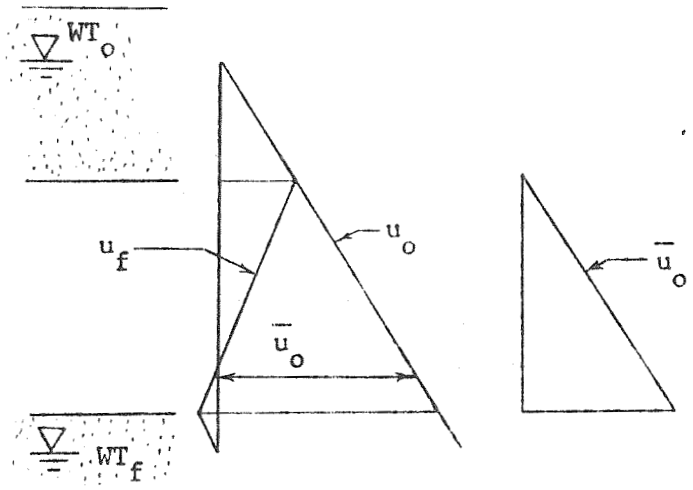

Case a: Triangular Stress Surface Caused by Instantly Dropping the Water Table in a Lower Drainage Layer to WT_f While Leaving the Water Table in the Upper Drainage Layer at WT_o

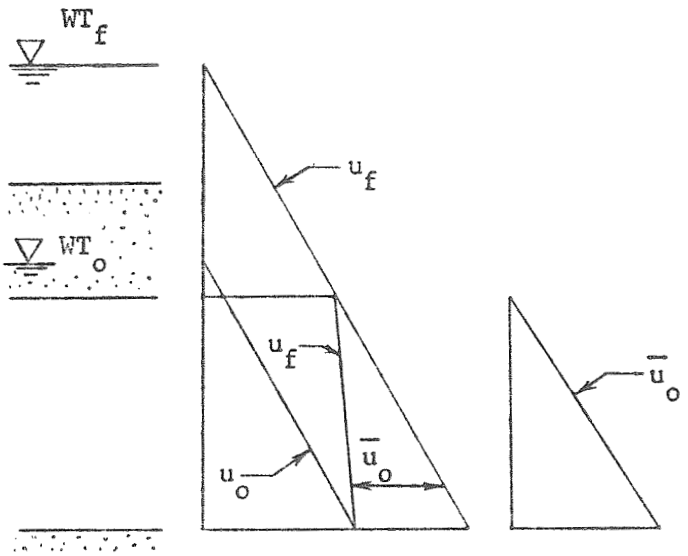

Case b: Triangular Stress Surface Caused by Instaneous Rise in the Water Table in the Upper Drainage Layer from WT_o to WT_f While Maintaining the Water Table for the Lower Drainage Layer at WT_o

Fig. 3.1 Examples of Triangular Stress Surfaces

from the apex of the triangular stress surface positively into the layer. The triangular stress surface extends entirely through the compressible layer and drainage is from both horizontal boundaries. The solution for excess pore water pressure is:

$$\bar{u} = \sum_{n=1}^{\infty} (2u_b/n\pi)(-1)^{n+1} \sin(n\pi z/2H) \exp(-n^2\pi^2 T/4) \quad . \quad . \quad . \quad . \quad . \quad . \quad (3.2)$$

The T-U relationship is again given by Eq. 2.5.

Trapezoidal stress surface. A trapezoidal stress surface is the sum of a rectangular stress surface and the triangular one just derived. Thus, no new set of equations need be derived.

Sinusoidal stress surface. The sinusoidal stress surface consists of a half sine wave, with a peak initial excess pore water pressure of u_s at mid-height and zero pore pressures at both boundaries (Fig. 3.2). The solutions for excess pore water pressure and the T-U relationship are:

$$\bar{u} = \bar{u}_s \sin(\pi z/2H) \exp(-\tfrac{1}{4}\pi^2 T) \quad . \quad . \quad . \quad . \quad . \quad . \quad . \quad . \quad . \quad (3.3)$$

and

$$U = 1 - \exp(-\tfrac{1}{4}\pi^2 T) \quad . \quad . \quad . \quad . \quad . \quad . \quad . \quad . \quad . \quad . \quad . \quad . \quad (3.4)$$

Composite stress surface. A simple solution can be obtained for a stress surface that is the sum of two stress surfaces, e.g., a rectangular stress surface from just applied fill and a sinusoidal stress surface from fill applied at some time previously. For a composite stress surface composed of N separate stress surfaces:

$$U = \sum_{j=1}^{N} U_j (A_j/A) \quad . \quad . \quad . \quad . \quad . \quad . \quad . \quad . \quad . \quad . \quad . \quad . \quad . \quad . \quad (3.5)$$

where j denotes any one stress surface, A_j is the area of the j-th stress surface, A is the area of the composite stress surface, and U_j is the average degree of consolidation for the j-th stress surface. The isochrones for the composite stress surface can, of course, be obtained simply by adding the excess pore pressures of each of the component stress surfaces at any given time.

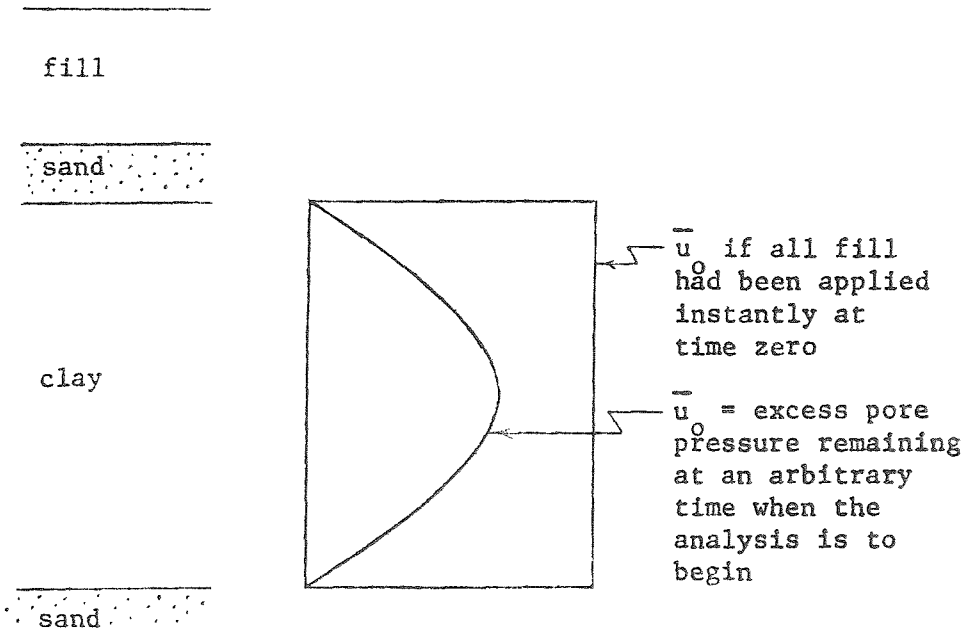

Fig. 3.2 Example of a Sinusoidal Stress Surface Generated by Gradual Application of Fill at an Irregular Rate During an Unknown Period of Time

Time-Dependent Loading

Loading is always time dependent but in some cases the loading time may be so short compared with consolidation times that instantaneous loading may be assumed. In the more general case we assume that the applied load, q, is any arbitrary function of time, t, such that a stress dq is applied during a time period dt (Fig. 3.3a). For the case of double drainage and a rectangular stress surface, the excess pore pressure ($d\bar{u}$) remaining in the soil at any time t due to an increment of pressure (dq) applied at time t_i is found from Eq. 2.5 to be:

$$d\bar{u} = \sum_{m=0}^{\infty} (2dq/M)\sin(Mz/H)\exp\{-M^2 c_v (t-t_i)/H^2\} \quad \ldots\ldots\ldots \quad (3.6)$$

A solution is obtained by expressing q as a function of t_i and integrating Eq. 3.6. The most useful solution is for a single ramp loading (Fig. 3.3b) in which the applied stress q increases linearly from zero at t=0 to q_c at time t_c, where t_c is conveniently termed the construction time. For times less than t_c the solution is:

$$\bar{u} = \sum_{m=0}^{\infty} (2q_c/M^3 T_c)\sin(Mz/H)\{1-\exp(-M^2 T)\} \quad \ldots\ldots\ldots \quad (3.7)$$

and:

$$U = (T/T_c)\left[1-(2/T)\sum^{\infty}(1/M^4)\{1-\exp(-M^2 T)\}\right] \quad \ldots\ldots\ldots \quad (3.8)$$

where T_c is the construction time factor defined as:

$$T_c = c_v t_c / H^2 \quad \ldots\ldots\ldots\ldots\ldots\ldots \quad (3.9)$$

For times in excess of t_c the solutions are:

$$\bar{u} = \sum_{m=0}^{\infty} (2q_c/M^3 T_c)\{\exp(M^2 T_c)-1\}\sin(Mz/H)\exp(-M^2 T) \quad \ldots\ldots \quad (3.10)$$

and:

$$U = 1 - (2/T_c)\sum_{m=0}^{\infty} (1/M^4)\{\exp(M^2 T_c)-1\}\exp(-M^2 T) \quad \ldots\ldots\ldots \quad (3.11)$$

Relationships between T and U for various construction time factors have been published (Olson, 1977).

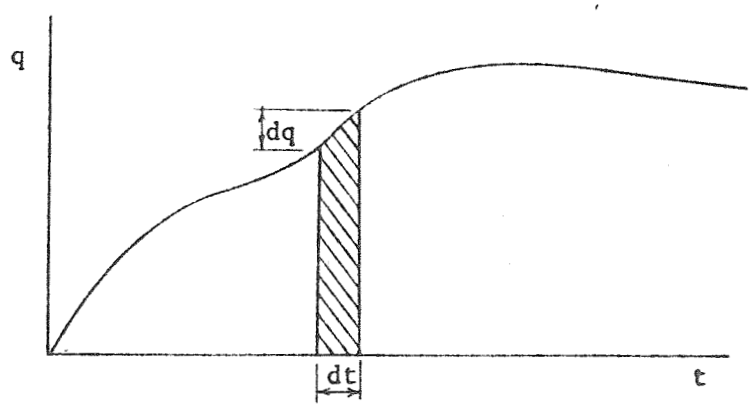

(a) Arbitrary Loading

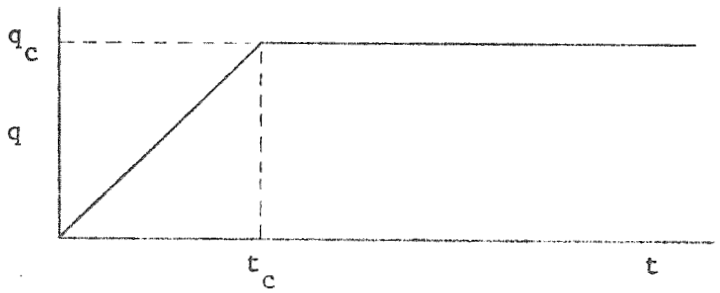

(b) Single Ramp Loading

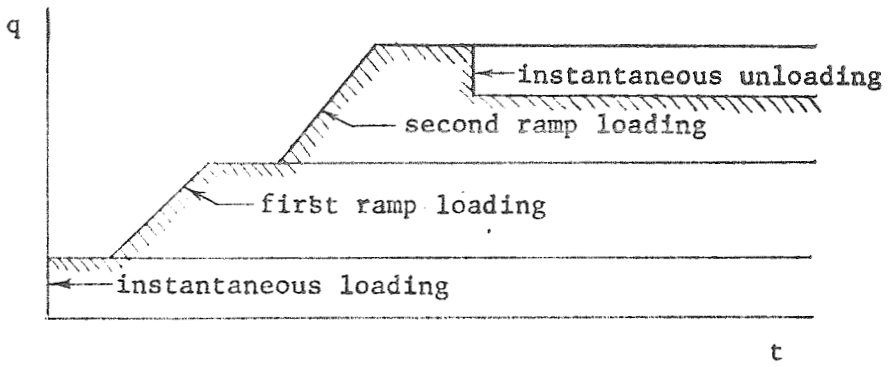

(c) Composite Loading

Fig. 3.3 Time Dependent Loading Diagrams

Solutions for most variations of loading or unloading can easily be obtained by approximating the actual loading with a series of instantaneous loadings or unloadings, and ramp loadings or unloadings (Fig. 3.3c). The equation for a composite stress surface (Eq. 3.5) may be proved to be valid for time dependent loading as well but now A_j is the area under the stress surface of the j-th loading (calculated as if this loading was applied instantaneously). The procedure was demonstrated by Olson (1977).

Impervious or Partially Draining Boundaries

The previous solutions were developed for the case that both horizontal boundaries of the compressible layer were freely draining. Solutions may be obtained for all previous cases with one or both boundaries either impervious or just partially draining.

Relatively impervious boundaries are often encountered in engineering practice but always with a rectangular stress surface. Since the mid-plane in the case of a doubly drained layer with rectangular stress surface, is a plane of symmetry, no flow occurs across this surface and the upper and lower halves of the double drained layer may be separately considered as layers with one freely draining boundary and one that is impervious. Thus, solutions presented previously in this section may be applied directly to obtain a solution. Solutions are easily derived for cases of non-rectangular stress surfaces but they seem to have no practical application and will not be reviewed.

In the case of partially draining boundaries, it is convenient to consider the soil layers next to the compressible layer as being incompressible but having low enough coefficients of permeability to hinder the free outflow of water from the compressible layer. Solutions are obtained by integrating Eq. 2.1 using the boundary conditions:

$$\partial\bar{u}(0,t)/\partial z = (R_2/L)\bar{u}(0,t) \quad . . . . . \quad (3.12)$$

$$\partial\bar{u}(L,t)/\partial z = (-R_1/L)\bar{u}(L,t) \quad . . . . . \quad (3.13)$$

and the initial conditions:

$$\bar{u}(z,0) = f(z) \quad . . . . . \quad (3.14)$$

where the notation (z,t) indicates the appropriate values of z and t for the pore pressure. The constants R_1 and R_2 are defined as:

$$R_1 = k_1 L/kH_1 \quad \ldots\ldots\ldots\ldots\ldots\ldots \quad (3.15)$$

$$R_2 = k_2 L/kH_2 \quad \ldots\ldots\ldots\ldots\ldots\ldots \quad (3.16)$$

where H_1 and H_2 are the total thicknesses of the lower and upper incompressible layers respectively, L is the thickness of the compressible layer, k_1 and k_2 are the coefficients of permeability of the lower and upper incompressible layers, respectively, and k is the coefficient of permeability of the compressible layer. The use of the parameters R_1 and R_2 was first suggested by Gray (1936). Use of a generalized Fourier series leads to the following solution:

$$\bar{u} = (1/L) \sum_{n=1}^{\infty} \exp(-r_n^2 T)\, D_n Z_n \int_0^L Z_n f(z)dz \quad \ldots\ldots\ldots \quad (3.17)$$

in which r_n represents successive positive roots, other than zero, of:

$$\tan(r_n) = r_n(R_1+R_2)/(r_n^2-R_1R_2) \quad \ldots\ldots\ldots\ldots\ldots \quad (3.18)$$

and:

$$D_n = 2(r_n^2+R_1^2)/\{(r_n^2+R_1^2)(r_n^2+R_2^2)+(r_n^2+R_1R_2)R_1+R_2)\} \quad \ldots\ldots\ldots \quad (3.19)$$

$$Z_n = r_n\cos(r_n z/L) + R_2\sin(r_n z/L) \quad \ldots\ldots\ldots\ldots\ldots \quad (3.20)$$

The simplest, and certainly most useful, solution is for the case of a constant initial excess pore water pressure $\bar{u}_o$:

$$\bar{u} = \bar{u}_o \sum_{n=1}^{\infty} D_n E_n Z_n \exp(-r_n^2 T) \quad \ldots\ldots\ldots\ldots\ldots \quad (3.21)$$

in which:

$$E_n = (1/r_n)\{r_n\sin(r_n)-R_2\cos(r_n)+R_2\} \quad \ldots\ldots\ldots \quad (3.22)$$

It is easily demonstrated that solutions to this problem published by Gray (1936) and Bishop and Gibson (1964) are special cases of Eq. 3.22. The T-U relationship is:

$$U = 1 - \sum_{n=1}^{\infty} D_n E_n^2 \exp(-r_n^2 T) \quad \ldots\ldots\ldots\ldots\ldots\ldots \quad (3.23)$$

Equations for other stress surfaces and for time-dependent loading are easily obtained but will not be presented.

Two Contiguous Compressible Layers

The solution for two contiguous compressible layers was published by Gray (1945). For the case of instantaneous loading, double drainage, uniform initial excess pore water pressure, small strains, constant properties, and linearly elastic and saturated soil, the T-U equations for layers 1 and 2 (interchangeable) are:

$$U_1 = 1 - 2 \sum_{n=1,2,..}^{\infty} \frac{\sin \xi A_n (\sigma \sin \xi A_n + \sin A_n)}{(A_n^2)(\sigma \sin^2 \xi A_n + \xi \sin^2 A_n)} (1 - \cos A_n) \exp(-A_n^2 T) \quad . \quad (3.24)$$

$$U_2 = 1 - \frac{2}{\xi} \sum_{n=1,2,..}^{\infty} \frac{\sin A_n (\sigma \sin \xi A_n + \sin A_n)}{(A_n^2)(\sigma \sin^2 \xi A_n + \xi \sin^2 A_n)} (1 - \cos \xi A_n) \exp(-A_n^2 T) \quad (3.25)$$

where A_n represents successive roots of:

$$\sigma \cos A_n \sin \xi A_n + \sin A_n \cos \xi A_n = 0 \quad \ldots\ldots\ldots\ldots \quad (3.26)$$

and:

$$\xi = \left(\frac{H_2}{H_1}\right) \left(\frac{c_{v1}}{c_{v2}}\right)^{\frac{1}{2}} \quad \ldots\ldots\ldots\ldots\ldots\ldots\ldots\ldots \quad (3.26)$$

$$\sigma = \left(\frac{k_1}{k_2}\right) \Big/ \left(\frac{c_{v1}}{c_{v2}}\right)^{\frac{1}{2}} \quad \ldots\ldots\ldots\ldots\ldots\ldots\ldots\ldots \quad (3.27)$$

$$T = c_{v1} \, t/H^2 \quad \ldots\ldots\ldots\ldots\ldots\ldots\ldots\ldots \quad (3.28)$$

where H_1 and H_2 are the total thicknesses of the two layers.

For the case of single drainage, the equations were derived with layer 1 defined to be the layer at the impervious boundary. The T-U relations are:

$$U_1 = 1 - 2 \sum_{n=1,2,..}^{\infty} \frac{\sin A_n \cos A_n \sin \xi A_n}{(A_n^2)(\sin^2 \xi A_n + \xi \cos^2 A_n)} \exp(-A_n^2 T) \quad \ldots\ldots \quad (3.30)$$

$$U_2 = 1 - \frac{2}{\xi} \sum_{n=1,2,..}^{\infty} \frac{\cos^2 A_n (1-\cos \xi A_n)}{(A_n^2)(\sigma \sin^2 \xi A_n + \xi \cos^2 A_n)} \exp(-A_n^2 T) \quad \ldots\ldots \quad (3.31)$$

where A_n represents successive roots:

$$\sigma \sin A_n \sin \xi A_n - \cos A_n \cos \xi A_n \quad \ldots\ldots\ldots\ldots \quad (3.32)$$

and other terms as defined above.

A solution for a system of many contiguous layers of compressible soil has been published by Schiffman and Stein (1970).

CHAPTER 4

LABORATORY OBSERVATIONS

Stress Strain Relationship

In Terzaghi's theory the assumption of linear elasticity is made in converting average degree of consolidation, U, to settlement (Eq. 2.10). If the soil is linearly elastic then the coefficient of compressibility, a_v, must be independent of effective stress, $\bar{\sigma}$. Relationships between a_v and $\bar{\sigma}$ are shown in Fig. 4.1 for a variety of soils. The assumption of constant a_v is reasonable if the change in effective stress during consolidation is small. Significant errors develop if the range in effective stress is large and includes the maximum previous consolidation pressure.

Variations in Coefficients of Consolidation

The coefficient of consolidation, c_v, is a derived soil property (Eq. 2.3) and is affected by variation in k, e, and a_v. Because all three vary with respect to effective stress, c_v is also likely to vary with respect to effective stress. For sensitive marine or lacustrine clays, k and e are relatively constant for stresses ($\bar{\sigma}$) less than the maximum previous consolidation pressure ($\bar{\sigma}_{max}$), and then decrease smoothly for higher effective stresses. The compressibility is typically very low during reloading ($\bar{\sigma} < \bar{\sigma}_{max}$), suddenly increases at $\bar{\sigma}$ near $\bar{\sigma}_{max}$, and then decreases smoothly again. As a result, c_v is typically high for reloading, decreases sharply at stresses near $\bar{\sigma}_{max}$, and then increases slowly for higher stresses (Fig. 4.2). The assumption of a constant coefficient of consolidation may thus be acceptable for only small ranges in effective stress provided that the range is not in the vicinity of $\bar{\sigma}_{max}$.

Secondary Effects

Secondary effects after primary consolidation. A typical curve of settlement versus logarithm of time, for a normally consolidated clay, is shown in Fig. 4.3. The dashed curve was calculated using Terzaghi's

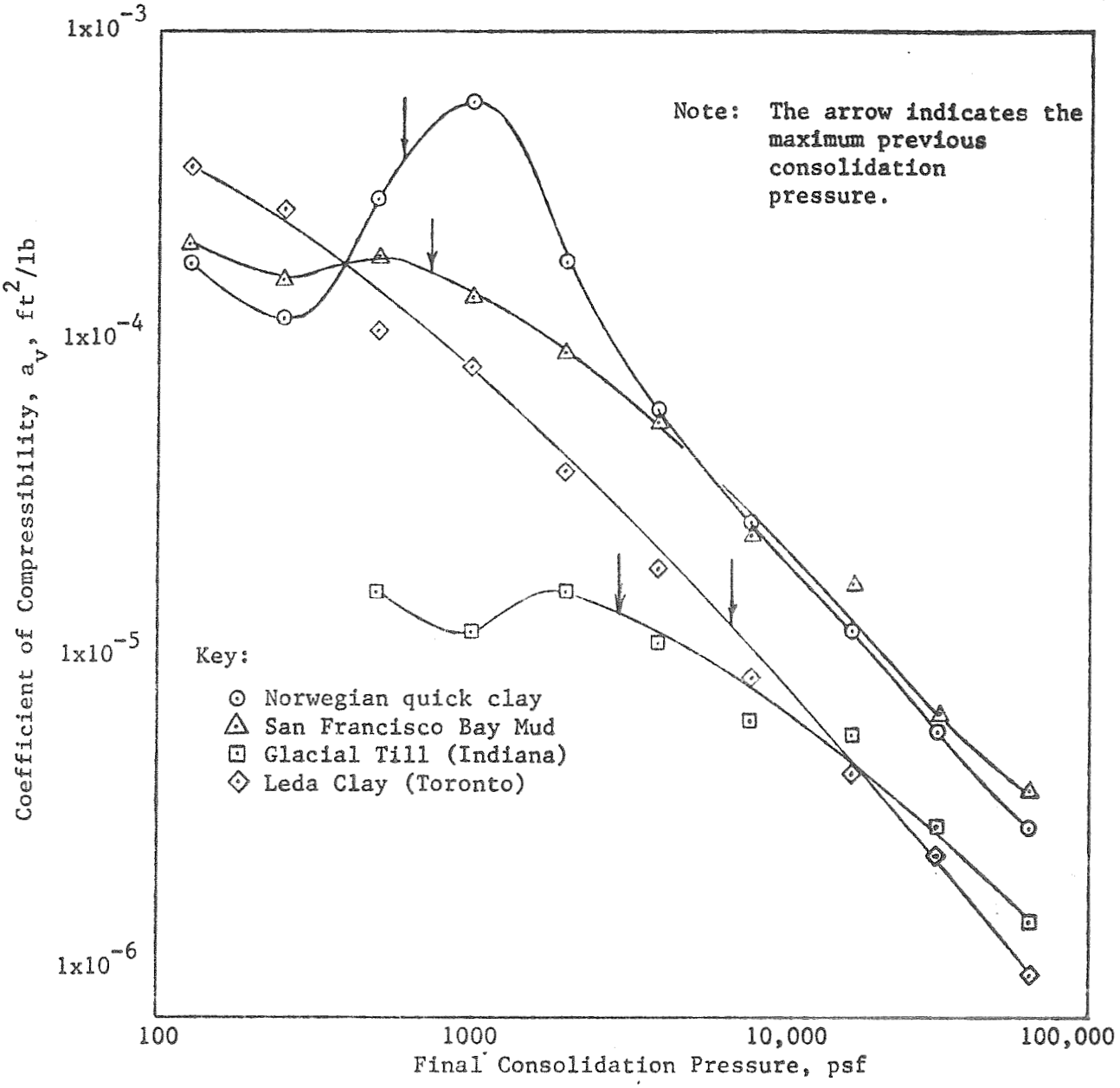

Fig. 4.1 Coefficients of Compressibility for Various Cohesive Soils. The coefficients have been plotted versus the final consolidation pressure for the load increment. The load-increment ratio was one. The highest coefficients always occur at the first pressure to lie on the virgin consolidation curve.

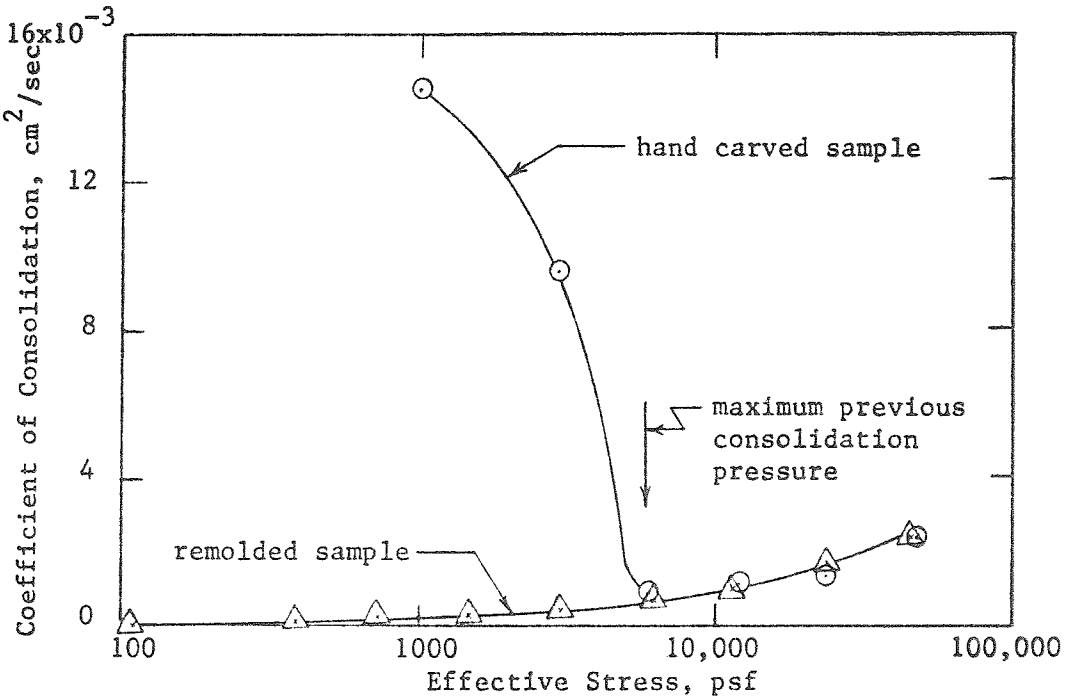

Fig. 4.2 Influence of Effective Stress on the Coefficient of Consolidation of Clay

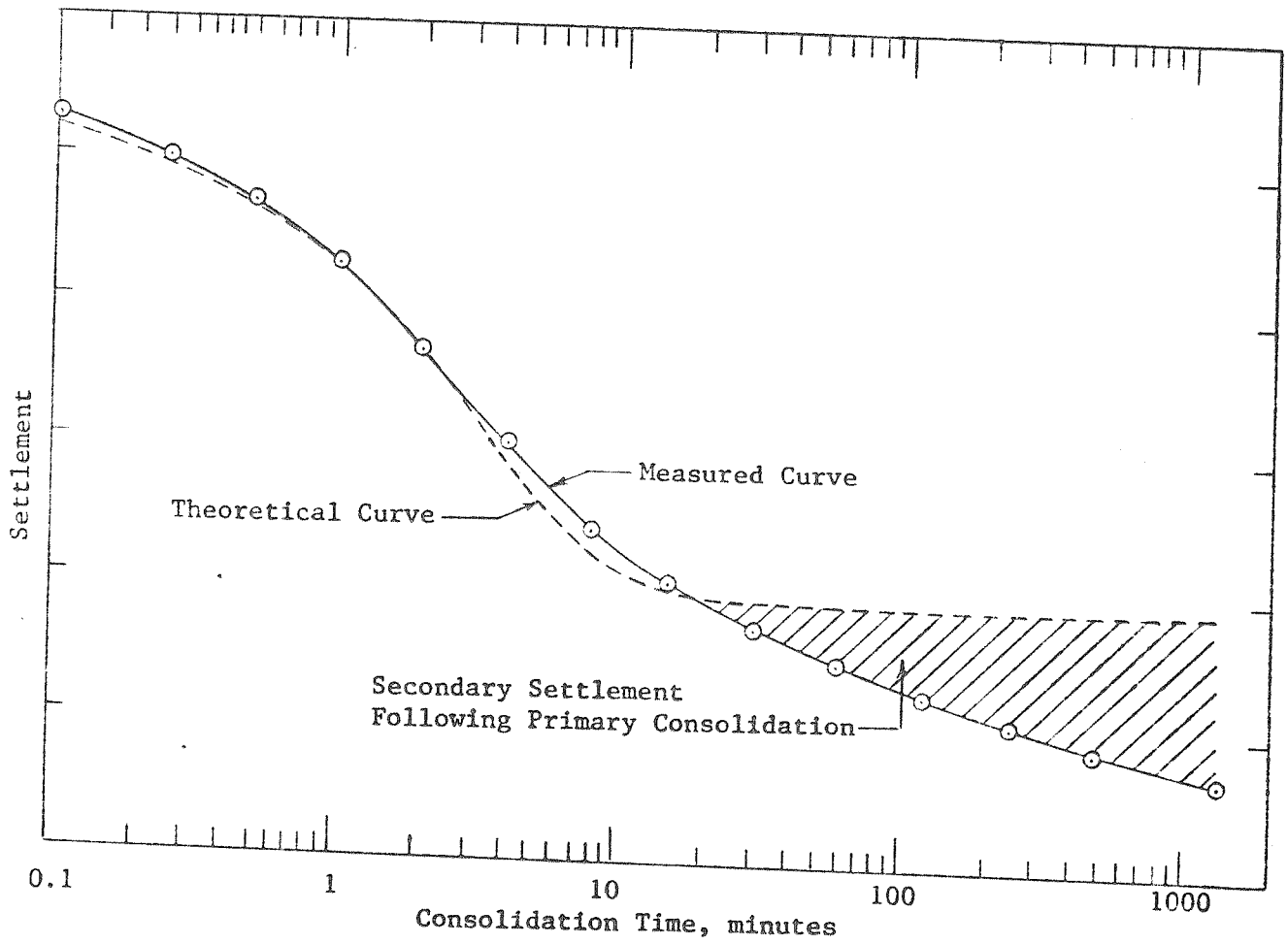

Fig. 4.3 Typical Relationship between Settlement and Logarithm of Time for a Normally Consolidated Clay

theory (Taylor, 1948, pp. 241-242). For this curve, 40% of the total settlement occurred after the completion of primary consolidation. Experience indicates that secondary settlements range from less than 10% to 100% of total settlement.

Most investigators find it convenient to assume that the curve of secondary settlement versus log of time is linear and define its slope as:

$$C_\alpha = de/d \log t \quad \text{(4.1)}$$

where e is void ratio and t is time. Mesri (1973) summarizes the various definitions that have been used for secondary slopes.

Linear secondary slopes have been observed in laboratory tests for up to seven years (Cox, 1936) but secondary slopes often increase with time when observations last only a few days (Thompson and Palmer, 1951; Lake, 1961; many others) but seem to diminish with time for most long term observations (Haefeli and Schaad, 1948; Lo, 1961).

Mesri (1973) summarized the effects of numerous variables on C_α, and provided extensive references to the literature. In general, C_α increases as the water content increases and is thus high for organic soils.

For undisturbed clays, C_α varies greatly with effective stress and peaks at a stress where the e - log $\bar{\sigma}$ curve assumes its greatest slope (Fig. 4.4).

The above observations indicate that a significant amount of settlement may occur after primary compression has been completed and that this additional settlement does not vary in any simple way with time.

In engineering practice, the primary S-t curve is typically analyzed using Terzaghi's theory and then the effects of post-primary secondary settlement is included simply by extending the theoretical S-log t curve at a slope C_α where C_α is the average value from laboratory tests at the appropriate effective stress.

Secondary effects during primary consolidation. The most obvious way of estimating whether or not Terzaghi's theory correctly models the consolidation process is to compare the shapes of laboratory S-t curves with reconstructed theoretical curves, as in Fig. 4.3. However, this comparison is relatively insensitive because the theoretical curve is constrained to

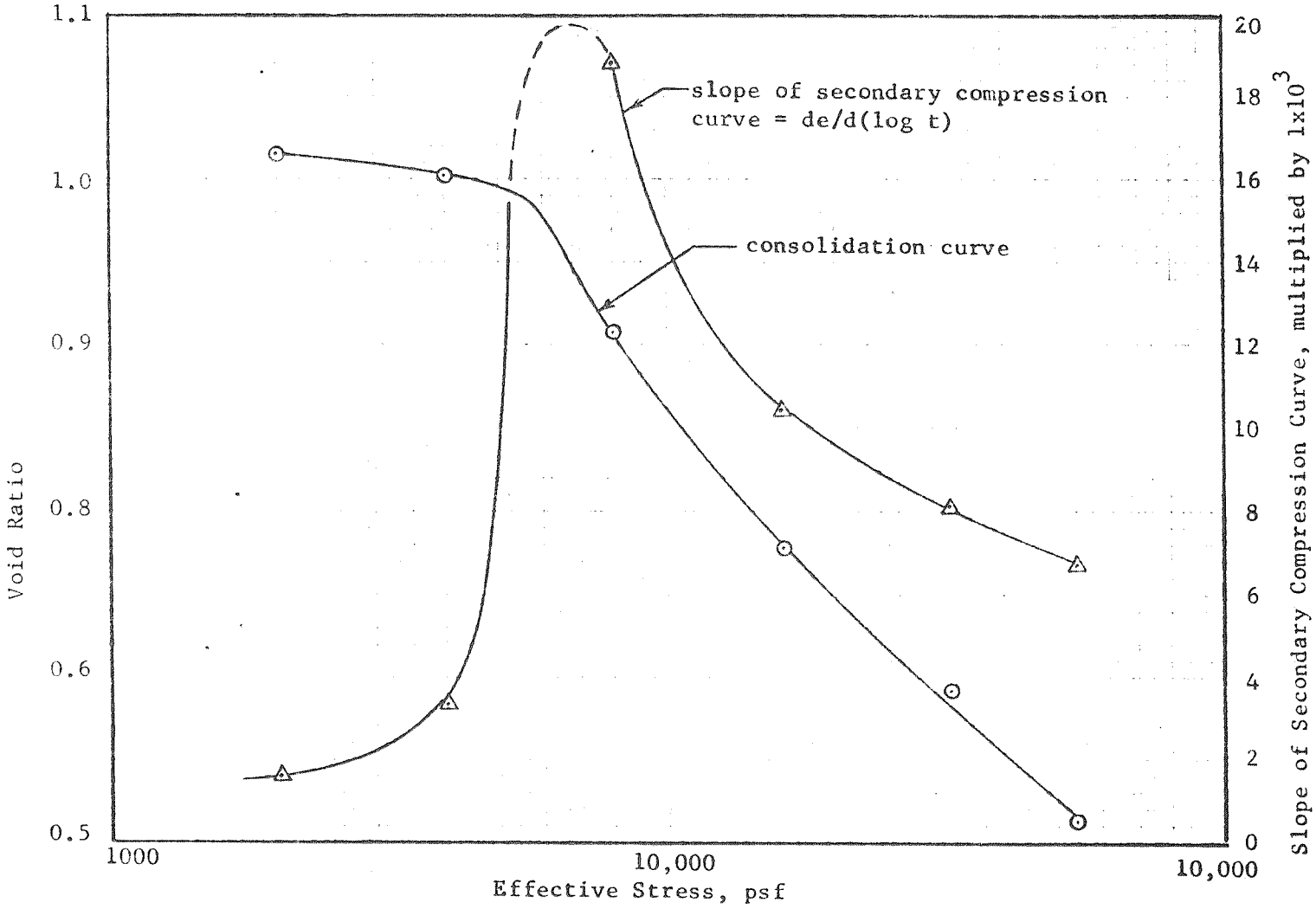

Fig. 4.4 Void Ratios and Slope of the Secondary Compression Curve for a Sample of Sensitive Leda Clay

have the same S_0 and S_{100} as the laboratory curve and to intersect the laboratory curve at the fitting point, typically at U = 50%.

A more sensitive method is to calculate the coefficient of permeability using Terzaghi's theory (Eq. 2.3) and to compare it with measured values by plotting both against void ratio. Terzaghi (1923b) and Casagrande and Fadum (1944) found excellent correlations between measured and computed permeabilities. Taylor (1942) found that the measured values were somewhat higher than theoretical values for Boston Clay. O'Neill (1954) found the measured values were up to ten times the theoretical values for undisturbed Boston clay, with the largest discrepancies during reloading. Typical data from our observations are shown in Fig. 4.5. Substantial discrepancies exist between measured and computed permeabilities during reloading but during virgin consolidation the two values differ by only about ten to forty percent, with the measured values higher.

The explanation of the above observations is as follows: The delay in consolidation is derived from two sources. The first is the delay resulting from finite permeability of the soil, the effect of which is included in Terzaghi's model. The second is a delay associated with the viscous resistance of the soil structure itself to volume change - the socalled secondary effects. Secondary effects retard consolidation during the primary stage. Because the only source of delay used in Terzaghi's theory comes from a low permeability, the extra delay caused by viscous resistance of the soil structure appears in his theory as an excessively low permeability.

The literature contains numerous papers in which models of combined primary and secondary effects are included. The only support for the models comes from comparisons of theoretical curves and the laboratory curves to which the theory was fitted. To our knowledge, there has never been published a comparison between a theoretical time-settlement curve, calculated using a combined primary/secondary theory, and a field measured time-settlement curve, where the parameters were obtained from laboratory tests. Further, the theories contain variables which have not been subject to independent measurement, as is the coefficient of permeability in Terzaghi's theory; thus, they are not even subject to independent laboratory measurement.

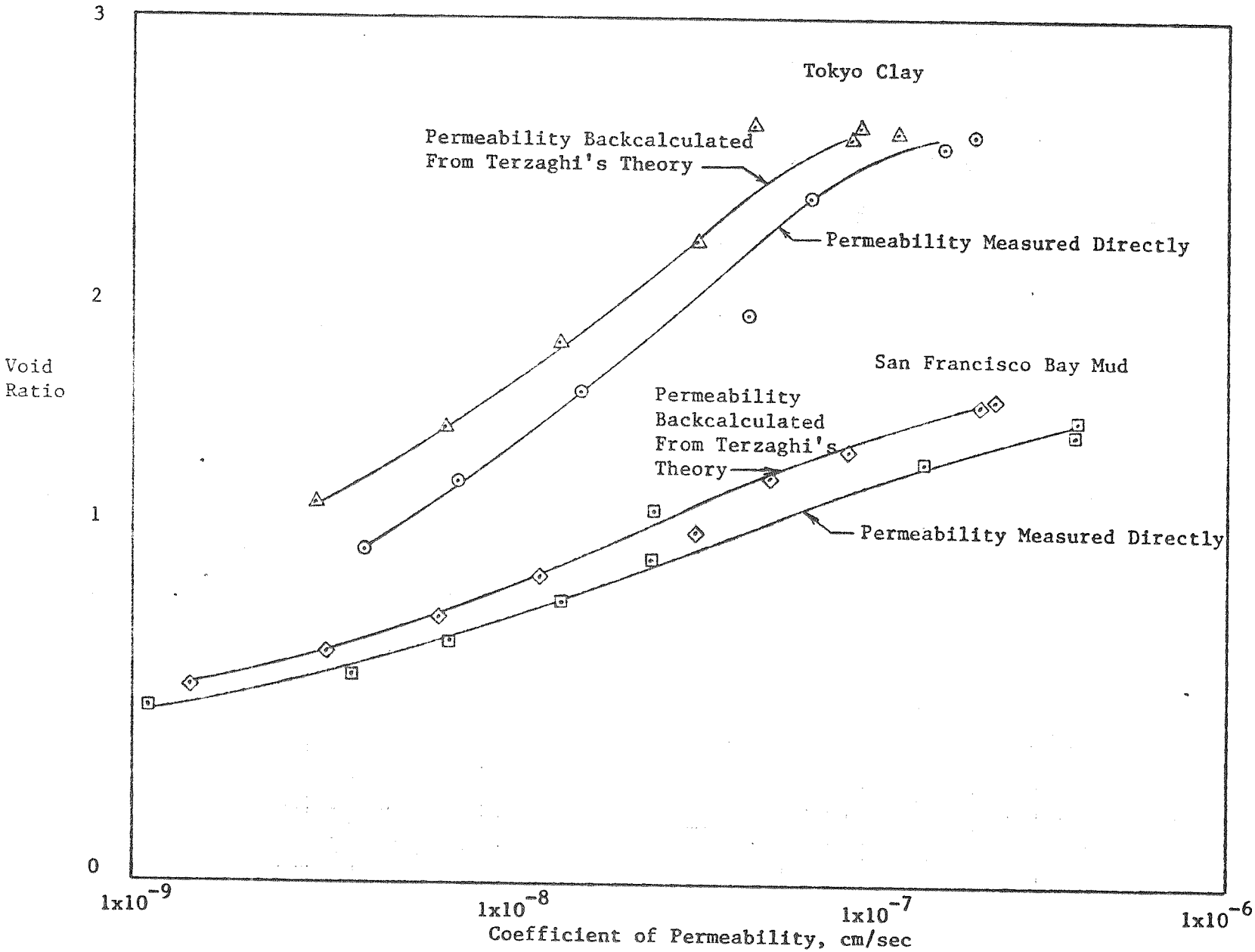

Fig. 4.5 Comparison of Coefficients of Permeability Measured Directly with Those Backcalculated From Time-Settlement Observations using Terzaghi's Theory

To our knowledge no primary/secondary theory has been applied to a field project during design. Because of the difficulty in making such analyses they are not likely to be used unless it can be demonstrated that an extended version of Terzaghi's theory cannot predict field behavior with acceptable accuracy.

CHAPTER 5

FIELD OBSERVATIONS

Time Dependent Loading

No real load of practical interest is ever applied instantly in the field. However, in some cases, the load application may be sufficiently rapid, or the soil sufficiently impervious, that the assumption of instantaneous loading is an acceptable approximation. An example might be the rapid filling of an oil storage tank with water to preload the subsoil.

A review of the literature reveals that rapid loading is more the exception than the rule, regardless of the type of structure involved. For instance, highway embankments are rarely constructed rapidly, as illustrated by over a half-dozen full-scale cases described in the literature that involve construction times which vary from 100 to 500 days and degrees of consolidation at the end of construction of from 50% to 90% (Samson and Garneau, 1973; Weber, 1968; Root, 1958; Kleiman, 1964; Henkel, 1965; Ortiz, 1966; Aldrich, 1965). Typical examples of time-dependent highway embankment construction are given in Fig. 5.1.

Construction of wide fills for site development in areas underlain by compressible soil is likewise rarely rapid. In two cases reported in the liaterature (Jonas, 1964; Kotzias and Stamatopoulos, 1969), construction times varied between 50 and 200 days while the degree of consolidation at the end of construction varied between 10% and 50%. Examples can also be cited of time-dependent loading of test fills (Herbert and Rowe, 1973; Murray, 1971) where construction times of 50 to 90 days resulted in up to 40% consolidation at the end of construction. Earth dams are usually built slowly as illustrated by Willard Dam where the construction time exceeded three years and the settlement during construction was over 10 feet (Walker, 1966).

A typical load-time curve for an oil storage tank preloaded with water is shown in Fig. 5.2 (Darrah, 1964). In a similar case, over 200 days

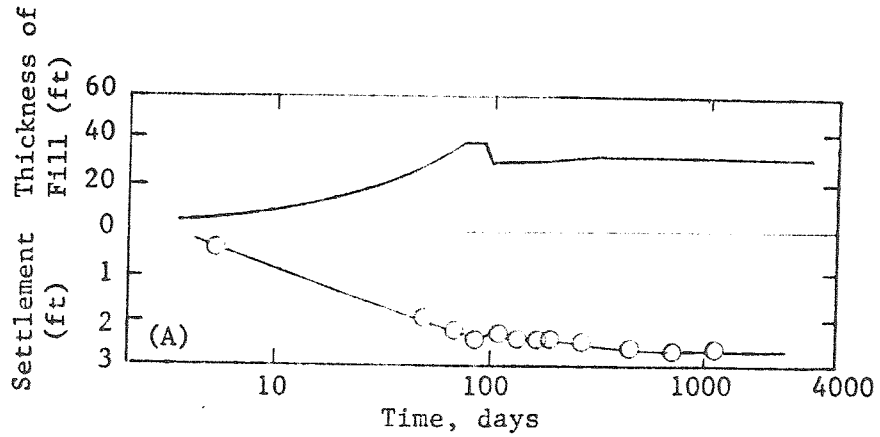

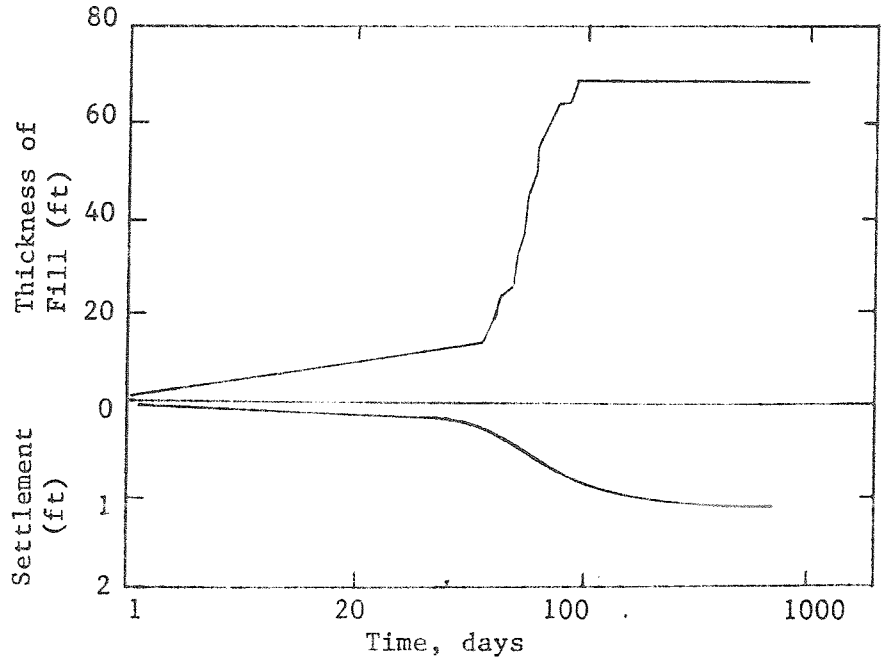

Fig. 5.1 Examples of Time-Dependent Highway Embankment Loading: (A) Atascadero Bypass, California (Weber, 1968); (B) Petaluma, California (Root, 1958)

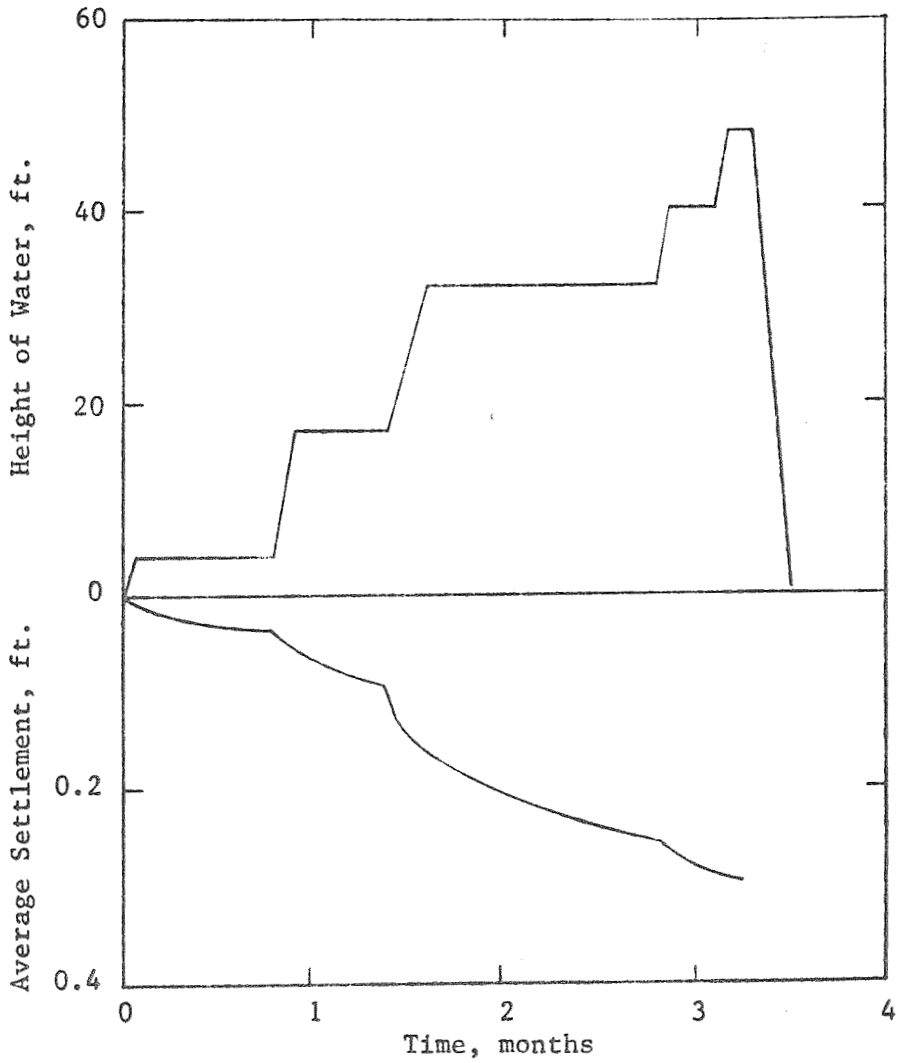

Fig. 5.2 Example of Time-Dependent Loading Involving Oil Storage Tank Preloaded with Water (Darragh, 1964)

were required to preload a storage tank fully and achieve most of the predicted settlement (Varghese and Ramanthan, 1971). In an example of relatively rapid loading of an oil tank (Gibson and Marsland, 1960), only three weeks were required to fill the tank; minimal consolidation occurred during this period. In a case history involving a grain silo (Nonveiller and Kleiner, 1969), filling the silo for the first time required 200 days, at which time 60% consolidation had been achieved.

Construction of buildings and bridges is rarely rapid. The state capitol building in California is thought to have settled about 12 inches during construction in the 1800's and to have required more than 10 years to build (Calif. Division of Highways). Of course, modern structures do not require such long construction times, although a few months is usually a minimum construction period even for small buildings while one to two years may be needed to load large buildings fully.

Bridge piers usually require several years to construct and load fully. For example, piers for the Waterloo Bridge were constructed on a deep deposit of London clay (Cooling, 1948); the time required to achieve full loading was four years and the degree of consolidation at the end of construction was approximately 60%.

Settlement-Dependent Loading

Except for the case of a completely immersed (underwater) fill, settlement of earthen structures is accompanied by a time-dependent reduction in effective load. Settlement-dependent loading is only of practical concern if the submergence correction is a significant percentage of the applied load. Some examples of cases reported in the literature where settlement-dependent loading did appear to be significant are given in Table 5.1. In one extreme case reported by Weber (1969, p. 68), a seven-foot-high embankment placed on a peat deposit actually settled 14 feet. In this case, if the water table was located at a depth of seven feet below original ground and remained at the same elevation during settlement, the submergence correction would be roughly equal to the applied load. Since Weber did not clearly state where the water table was

Table 5.1 Example of Cases Where Settlement-Dependent Loading Was Significant

Reference	Project Location	Description of Compressible Soil	w(%)	LL(%)	PL(%)	Fill Thickness (ft)	Settlement (ft)	Approx. Change in Effective Load Due to Settlement
Samson & Garneau (1973)	Montreal	Silty Clay	50	60	30	35	7	10%
Root (1958)	Oakland, CA	Soft Clay	--	--	--	30	7	12%
Root (1958)	Antioch, CA	Peat	600	--	--	15	12	40%
Root (1958)	California	Peat over Soft Clay	500-800 (peat)	--	--	15	18	50% to 60%
Henkel (1965)	Lagos, Nigeria	Soft Organic Clay	180	200	80	15	10	33%
Walker (1966)	Willard, Utah	Organic Silt	50	50	20	40	11	14%
McAlpin & Sinacori (1955)	Syracuse, N.Y.	Marl, Silt and Clay	50-80	50	30	25	10	20%
Tsien (1955)	Red Bank, N.J.	Organic Silt with Peat	190-570	--	--	35	20	29%
Weber (1969)	Antioch, CA	Peat Over Silty Clay	150-600	--	--	7	14	50% to 100%
Weber (1966)	Napa, CA	Soft Silty Clay	85	87	38	32	13	20%
Cedergren & Weber (1962)	San Francisco	Soft Silty Clay	--	--	--	7.5	4	27%
Cedergren & Weber (1962)	Tule Lake, CA	Soft Silty Clay	--	--	--	23	18	40%
Rafaeli (1972)	Norfolk, VA	Soft Clay	40	40	20	41	13	16%

located in this particular case, it is not certain the submergence correction was as large as 100% of the original applied load, although it seems almost certain it was at least 50%. As one can see from Table 5.1, at least a half-dozen less extreme examples can be given of cases where the submergence correction was 25% or more of the original applied load. Clearly, where settlements are large, a submergence correction is needed if substantial errors in both the computed total and time-rate of settlement are to be avoided.

Fluctuations in the Position of the Water Table

Anytime the position of the water table changes within a mass of soil, the effective load on the underlying soil also changes.

Several case histories can be cited to illustrate instances where changes in the position of the water table had a significant effect on field performance. Kotzias and Stamatopoulos (1969) report seasonal fluctuations in the water table of five feet at a site in Greece that was preloaded to permit construction of a heavy industrial installation on shallow foundations bearing on compacted fill. The change in applied effective load due to water table fluctuation (about 300 psf) was equal to 20% of the soil preload (about 1500 psf). In this case the water table was highest in February-March and lowest in September-October. Similarly, Wallace and Otto (1964) observed five-foot seasonal fluctuations in the water table at Selfridge Air Force Base, Michigan. In this case the change in effective load due to water table fluctuation was a large percentage of the load caused by one-story structures and it was observed that the buildings on the air base seemed to rise and settle according to variations in the position of the water table. In these two examples, failure to account for seasonal fluctuations in the water table would have led to significant error in predicted performance.

Fluctuations in river stages may have a significant effect on groundwater levels adjacent to a river. At one industrial plant along the south shore of the St. Lawrence River east of Montreal fluctuations in the river stage of 18 feet seemed to have had a noticeable effect on settlement of the industrial site (Casagrande, Firing, Schoof and Turcke, 1965). Similar

fluctuations were noted near New Orleans where piers supporting a highway bridge across the Mississippi River settled and later rebounded in accordance with changes in the river stage (Kimball, 1936). At a site near Bangkok seasonal flooding raised ground water levels five feet in a 10-foot-high flood protection levee, thus causing a 25% reduction in applied effective load (Moh, Brand, and Nelson, 1974).

At least three examples can be given of cases where the construction of earth fills on soft ground created excess pore water pressures in the foundation soils that were sufficient to cause the water table to rise into the earth fill (Tsien, 1955; Burn, 1969; Webber and Hill, 1955). In one case, the water table rose ten feet into an embankment (Webber and Hill, 1955).

Other examples of time-dependent variations in the position of the water table include wide-spread settlement caused by pumping from a deep aquifer (Lambe, 1969) and settlement caused by drawdown of the water table in connection with dewatering a deep excavation (Hutchinson, 1964).

Stratified Soils

Few natural deposits of soil are unstratified. Stratifications may be nearly microscopic (for example, in some marine deposits such as San Francisco Bay mud), may be visible to the naked eye (for instance, in varved lacustrine soils), or may be several feet or more in thickness and discernable from borehole logs (for example, many alluvial soils contain distinctly different strata of compressible soil).

There are many examples of structures built over stratified deposits of compressible soil. Kuesel, Schmidt, and Rafaeli (1973) describe a two-layer system of compressible soil beneath a fill island in Virginia. Three-layer systems have been reported beneath a building (Crawford and Sutherland, 1971), a test embankment (Justo, 1969), and a highway embankment (Stermac, Lo, and Barsvary, 1967). Similarly, four layer systems have been described beneath an embankment (McAlpin and Sinacori, 1955) and a test fill (Chang, Broms and Peck, 1973). Kaufman and Sherman (1964) report engineering measurements for Port Allen Lock which was underlain by five layers of compressible silt or clay. Moore and Grosert (1968)

describe field performance of a highway embankment built over six distinct layers of silt, clay, peat, or sludge. An extreme example of layered soils is in the vicinity of the Atchafalaya flood protection levees in Louisiana where 12 distinct compressible strata can be found at some locations (U.S. Army Corps of Engineers, 1968).

Large Strains

Practical field cases sometimes involve large strains. As indicated in Table 5.2, strains of 20% or more are not uncommon and, in one case, a strain of over 70% was reported.

Non-Linear Stress-Settlement Relationships

Several investigators have reported field stress-settlement relationships, either in the form of a void ratio-effective stress curve (Root, 1958; Varghese and Ramanthan, 1971; Miyahara, Nakamura and Takayama, 1967; Schmidt and Gould, 1968; Wu and Peck, 1956), or a vertical strain-effective stress curve (Ladd, Rixner and Gifford 1972). For virgin compression, the field data clearly show that void ratio is not a linear function of effective stress, but rather, is approximately a linear function of the logarithm of effective stress. In fact the field stress-settlement curves follow the general shape of non-linear laboratory stress-settlement curves measured in one-dimensional consolidation tests. For example, Ladd, Rixner, and Gifford (1972) published the field and laboratory stress-settlement curves shown in Fig. 5.3. To illustrate the non-linearity of field stress-strain behavior, the left-most field curve in Fig. 5.3 is replotted in Fig. 5.4 with a natural scale for effective stress. Also shown in Fig. 5.4 is the linearly elastic behavior that would be assumed in a closed-form analysis.

Stress Dependent Coefficients of Permeability

For analytical purposes the stress dependency of the coefficient of consolidation is of interest but this parameter is not subject to direct field measurement. Coefficients of permeability can be measured directly

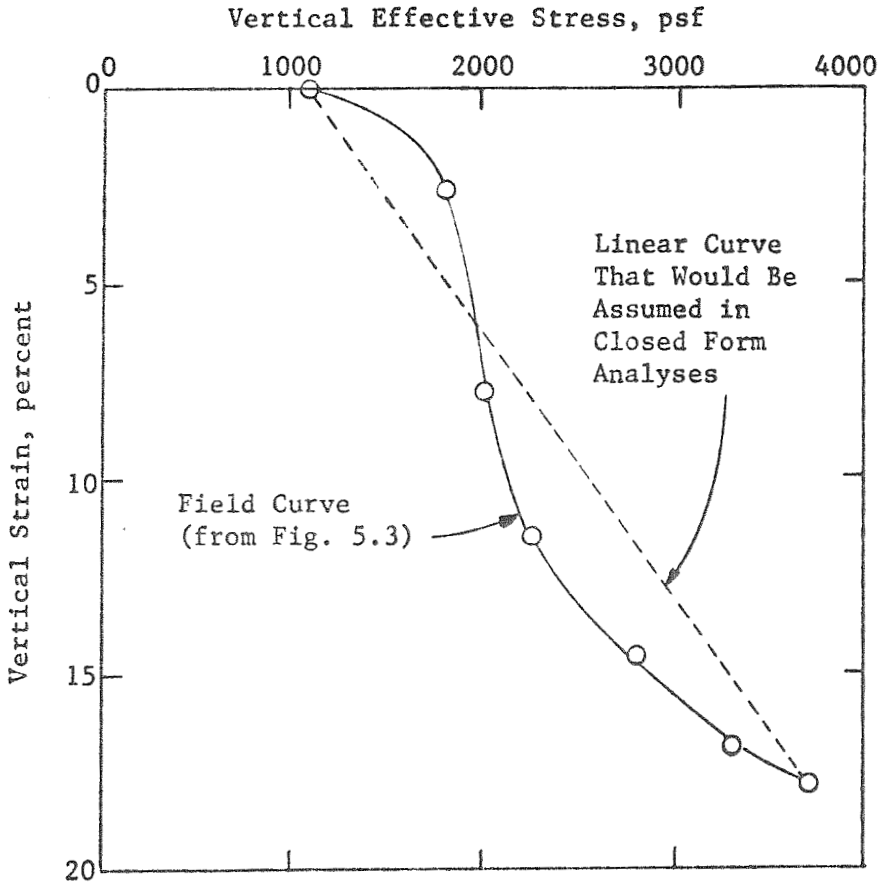

Fig. 5.4 Non-Linear Stress-Settlement Curve Replotted from Fig. 5.3

in the field and when coupled with compressibilities can be used to infer changes in the coefficient of consolidation.

Weber (1969) was apparently the first to describe changes in in-situ permeability during consolidation. He found 1000 fold decreases in permeability of peat deposits underlying three highway embankments in California. James (1970) describes in-situ measurements of permeability beneath two full-scale trial embankments constructed in Malaya over soft, silty clay. He found that permeability decreased by 50% during the six months following construction.

Murray (1971) reports measurements of in-situ permeability beneath Avonmouth test embankment, which was underlain by three distinct layers of clay and a stratum of peat. His data, shown in Fig. 5.5, indicate decreases in field permeability of the order of 5 to 50 fold over a period of three years.

Effective Stress Dependent Coefficients of Consolidation

Coefficients of consolidation can be backcalculated by trial-and-error fitting of theoretical curves to field settlement-time curves but the lack of a suitable closed form theory taking into account the effects already documented makes this method difficult to apply. Further, if only surface settlements are known, there will usually be an insufficient number of observations to isolate all effects.

A method originated by Gould (1949) has been used to obtain estimates of field c_v values. Gould applies Eq. 2.7 to a short time period Δt to obtain:

$$c_v = \frac{\Delta T}{\Delta t} H^2 \quad \ldots\ldots\ldots\ldots\ldots\ldots \quad (5.1)$$

Gould estimates ΔT from the Terzaghi T-U relationship (Eq. 2.9) using input values of U defined from Eq. 2.10. The method has actually been applied to sand drain projects using c_h and R_e in place of c_v and H but the concept remains the same.

Published data on values of $\tilde{c}_v = c_h$ obtained by fitting theoretical curves to field curves or using Gould's method indicate decreases in the

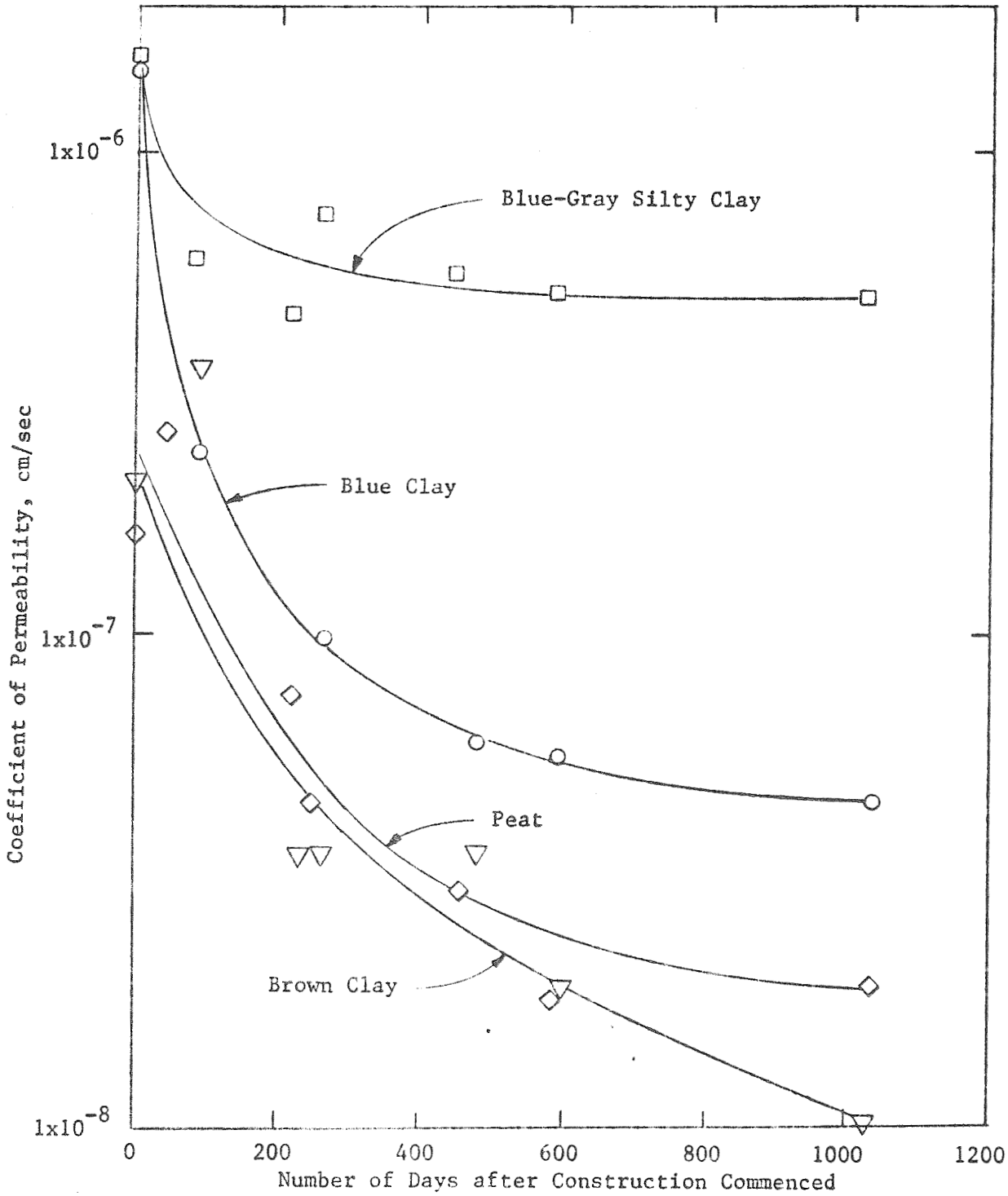

Fig. 5.5 Decrease in Field Permeability Beneath Avonmouth Test Embankment (Murray, 1971)

coefficient of consolidation of about two to ten times (Kuesel, Schmidt and Rafaeli, 1973; Aboshi and Mondin, 1963; Lindskog and Broms, 1970; Holtz and Lindskog, 1972; Moran et al., 1958, N.Y. 3.1) although Herbert and Rowe (1973) found a reduction of 1000 times.

Closure on Field and Laboratory Observations

The field and laboratory observations just reviewed, and many others not reviewed, make it clear that the assumptions included in the classical theory of consolidation do not describe, accurately, conditions that actually exist on real projects. Further, there is a strange lack of field evidence in support of the theory, considering that it has been in extensive use for more than forty years. We believe that the lack of supporting field evidence results from: (1) lack of a theory that reasonably accounts for all known major variables, (2) sampling techniques and laboratory testing methods that yield erroneous soil properties, (3) inadequate data on field stratigraphy, and (4) lack of field measurements. The lack of an appropriate theory is probably the major problem in that there is little point in working out detailed stratigraphy and soil properties if they cannot be used.

The remainder of this report will cover the finite difference method of analysis, and particularly a program FD31.

CHAPTER 6

FINITE DIFFERENCE METHOD OF ANALYSIS

Introduction

Most, if not all, of the simplifying assumptions of Terzaghi's theory can be generalized through use of a numerical method of analysis in which a digital computer is used to integrate the equations in suitably small steps and thus obtain solutions that approach exact solutions as the size of the steps diminish. Such assumptions as constant properties, small strains, and homogeneous material may be made for a single step, either spatially or in time, but a new set of conditions may be used for the next step, thus making it possible to vary conditions in a way that is impossible in closed form solutions. The problem, then, becomes one of developing an algorithm that takes into account all significant variables and achieves a tolerably accurate solution using a reasonable amount of computer time.

For consolidation problems both the finite difference and finite element methods of analysis may be used. It appears that the finite difference method is more efficient (Desai and Johnson, 1973; Schiffman, 1972) and it is very much simpler for one-dimensional problems in terms of the mathematics.

Previous Work with Finite Differences

The finite difference method has been used extensively in many fields of technology and science and is covered in a number of books and hundreds of papers. The first application of the method to the consolidation problem appears to have been by Gibson and Lumb (1953) although Scott (1953) used the method simultaneously in an unpublished thesis. Subsequently, Richart (1957) extended the method from one dimensional vertical consolidation to two-dimensional consolidation around sand drains, and Abbott (1960) introduced the more sophisticated Crank-Nicholson method of analysis. In the United States two computer programs were written to solve one dimensional consolidation problems and were made widely available. The

first, SEPOL-I, was based on the explicit method of analysis (Schiffman and Whitman, 1966; Schiffman, Whitman, and Jordan, 1970), and the second, PROGRS-I, on the Crank-Nicholson method (Schiffman and Stein, 1969). Both programs take into account time dependent loading and stratified soils. Subsequently, Olson, Daniel, and Liu (1974) developed a sophisticated program for analysis of sand drain problems and Olson and Ladd (1977) reported on a more advanced program for one-dimensional problems.

Definition of Difference Equations

The finite difference method is a technique for integrating differential equations. It makes use of three types of differences which are termed forward differences, central differences, and backward differences, and each comes in a series of orders, e.g., first forward difference, second forward difference, ... Only the first forward difference, and the first and second central differences will be considered in this report.

The difference equations are used to integrate a dependent variable in terms of one or more independent variables. To preserve generality and simplify subscripting for the moment, we will use y for the dependent variable (subsequently the dependent variable will be $\bar{u}$) and x for the independent variable (subsequently to or z). We assume that y is some function of x, as indicated in Fig. 6.1. Because we are working with finite differences rather than differentials, we assume that the variable y is known only at discrete points denoted by .... x_{i-2}, x_{i-1}, x_i, x_{i+1}, x_{i+2}, ... where i denotes an arbitrary point on the x axis from which we wish to develop the difference equations.

First forward difference. The symbol Δ is used to indicate forward differences. The first forward difference is defined as:

$$\Delta y_i \equiv y_{i+1} - y_i \quad \ldots\ldots\ldots\ldots\ldots\ldots \quad (6.1)$$

If all derivatives of y are known at point i then a Taylor series can be used to find y_{i+1}:

$$y_{i+1} = y_i + \frac{\Delta x}{1!} y' + \frac{(\Delta x)^2}{2!} y'' + \frac{(\Delta x)^3}{3!} y''' + \ldots\ldots$$

$$\frac{(\Delta x)^n}{n!} y^{n'} + \ldots\ldots\ldots\ldots\ldots\ldots\ldots\ldots \quad (6.2)$$

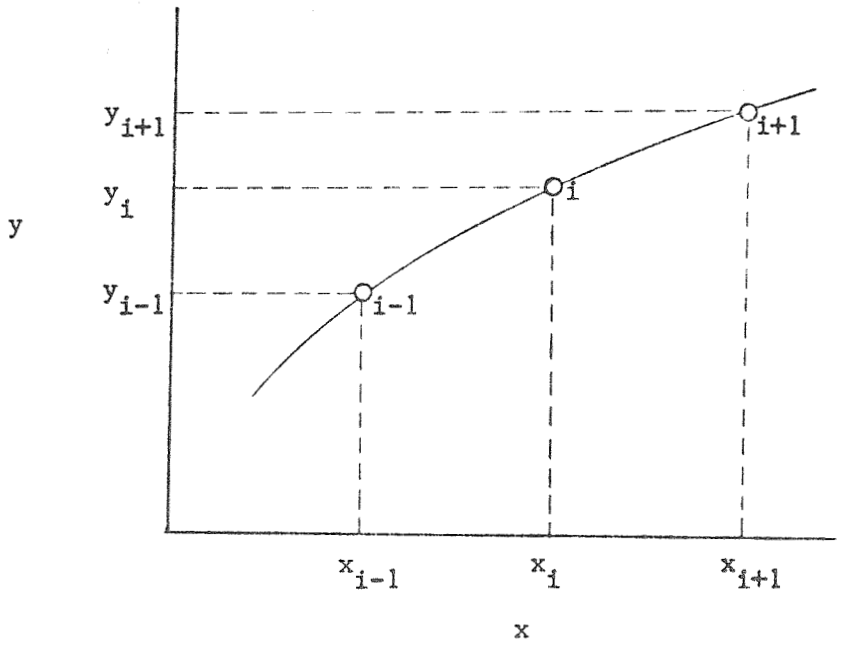

Fig. 6.1 Definition of Nodes for Use in the Finite Difference Method

where y' indicates dy/dx, y'' indicates d^2y/dx^2, etc., and Δx is the spacing of points along the x axis.

As a first approximation, we assume that the spacing Δx is so small that a sufficiently accurate value of y_{i+1} can be obtained by truncating the series after the y_i' term. Thus:

$$\Delta y_i = y_{i+1} - y_i \sim (y_i + \frac{\Delta x}{1!} y') - y_i = \Delta x\, y_i' \quad \ldots\ldots\ldots \quad (6.3)$$

Thus, a first approximation for y_i' is:

$$\Delta y_i' = dy/dx = (y_{i+1} - y_i)/\Delta x \quad \ldots\ldots\ldots\ldots\ldots \quad (6.4)$$

First averaged central difference. The symbol δ is used as the central difference operator. Thus, the first central difference is defined as:

$$\delta y_i = y_{i+\frac{1}{2}} - y_{i-\frac{1}{2}} \quad \ldots\ldots\ldots\ldots\ldots \quad (6.5)$$

This rather strange definition results from the fact that the differences are defined over an interval Δx. Because the function y is defined at only discrete points, it is necessary to replace $y_{i+\frac{1}{2}}$ by $\frac{1}{2}(y_{i+1} + y_i)$ and $y_{i-\frac{1}{2}}$ by $\frac{1}{2}(y_i + y_{i-1})$ to make Eq. 6.5 appear as the first averaged central difference:

$$\delta y_i = \tfrac{1}{2}(y_{i+1} - y_{i-1}) \quad \ldots\ldots\ldots\ldots\ldots \quad (6.6)$$

The Taylor series is applied as before and is again truncated after the y_i' term to obtain:

$$y_i' = (y_{i+1} - y_{i-1})/2\Delta x \quad \ldots\ldots\ldots\ldots\ldots \quad (6.7)$$

Equation 6.7 is the first averaged central difference approximation for the first derivative.

Second central difference. The central difference operator is applied again to obtain:

$$\delta^2 y_i = \delta(\delta y_i) = \delta(y_{i+\frac{1}{2}} - y_{i-\frac{1}{2}}) = \delta y_{i+\frac{1}{2}} - \delta y_{i-\frac{1}{2}} =$$

$$y_{i+1} - 2y_i + y_{i-1} \quad \ldots\ldots\ldots\ldots\ldots \quad (6.8)$$

The Taylor series is again applied to evaluate y_{i+1} and y_{i-1} but this time the y_i' terms disappear and the series is truncated after the y_i'' term. The resulting equation is solved for y_i'' to obtain:

$$y_i'' = d^2y/dx^2 \sim (y_{i+1} - 2y_i + y_{i-1})/(\Delta x)^2 \quad \ldots\ldots\ldots \quad (6.9)$$

Equation 6.9 is the second central difference approximation for the second derivative of y with respect to x.

Variations. The foregoing analysis may be extended to include higher order approximations but such analyses have not proved useful for the types of problems of interest here and will not be pursued.

Explicit Method

In this section, consideration will be restricted to a problem for which Terzaghi's theory is applicable. Terzaghi's differential equation of consolidation (Eq. 2.1) will be approximated using finite differences by replacing $\partial\bar{u}/\partial t$ by the first forward difference approximation, and $\partial^2\bar{u}/\partial z^2$ with the second central difference approximation to obtain:

$$\frac{\bar{u}_{z,t+\Delta t} - \bar{u}_{z,t}}{\Delta t} = c_v \frac{\bar{u}_{z+\Delta z,t} - 2\bar{u}_{z,t} + \bar{u}_{z-\Delta z,t}}{(\Delta z)^2} \quad \ldots\ldots\ldots \quad (6.10)$$

where the i-th point is now indicated as the (z,t) point, and the i+1 point on the time axis is $t+\Delta t$, and the i-1 and i+1 points on the depth axis are the $z-\Delta z$ and $z+\Delta z$ points, respectively.

As indicated previously, the finite difference equation is used to define the dependent variable, $\bar{u}$, at specific points rather than continuously. The equation will thus be satisfied at a series of points, termed nodes, which are distributed uniformly with respect to depth and time (Fig. 6.2) at spacings of Δz and Δt, respectively. Thus, Eq. 6.10 must be applied at each node in such a way that all of the pore pressures can be calculated. All of the pore pressures are known at time zero (the socalled initial conditions) and must also be defined at both boundaries (boundary conditions).

Equation 6.10 is first applied with t=0; thus every pore pressure with a subscript "t" is known and the only unknown pore pressure in Eq. 6.10

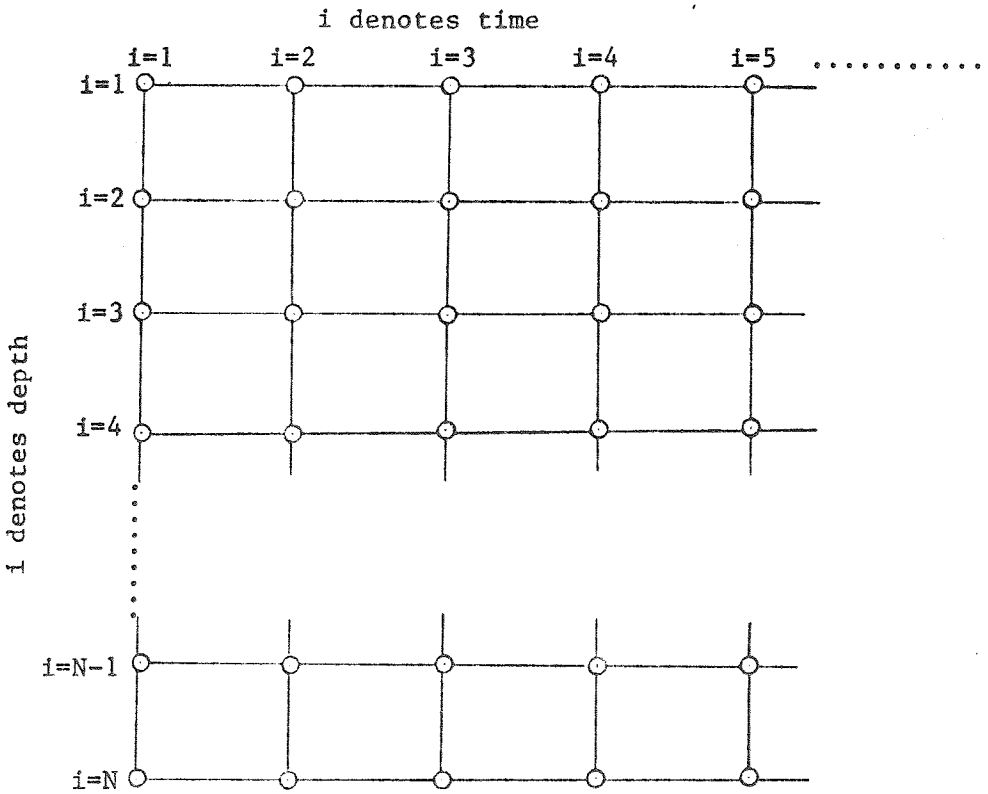

Fig. 6.2 Distribution of Nodes with Respect to Depth and Time

is $\bar{u}_{z,t+\Delta t}$. Equation 6.10 is solved for this pore pressure to obtain:

$$\bar{u}_{z,t+\Delta t} = \bar{u}_{z,t} + (c_v \Delta t/\Delta z^2)(\bar{u}_{z-\Delta z,t} - 2\bar{u}_{z,t} + \bar{u}_{z+\Delta z,t}) \quad . \quad . \quad . \quad . \quad . \quad . \quad (6.11)$$

Equation 6.11 may be applied to each node at time $t+\Delta t$ so that all of the pore pressures at that time become known. Those pore pressures then become the ones at time t and the pore pressures at the next time $t+\Delta t$ are calculated. The process is continued until all pore pressures have dissipated.

In the analyses it is convenient to replace $(c_v \Delta t/\Delta z^2)$ with the symbol α. Error analysis and experience both show that a stable solution will only be obtained with the explicit method if α is smaller than, or equal to, 0.50.

In making a solution to demonstrate application of Eq. 6.11, it is convenient to note from the definition of the time factor, T (Eq. 2.7), that:

$$\Delta t = c_v \Delta T/H^2 \quad . \quad . \quad . \quad . \quad . \quad . \quad . \quad . \quad . \quad . \quad . \quad . \quad . \quad . \quad (6.12)$$

and that introduction of:

$$\zeta = z/H \quad . \quad . \quad . \quad . \quad . \quad . \quad . \quad . \quad . \quad . \quad . \quad . \quad . \quad . \quad . \quad . \quad . \quad . \quad (6.13)$$

reduces the equation for α to:

$$\alpha = \Delta T/\Delta \zeta^2 \quad . \quad . \quad . \quad . \quad . \quad . \quad . \quad . \quad . \quad . \quad . \quad . \quad . \quad . \quad . \quad . \quad . \quad . \quad (6.14)$$

A hand solution is conveniently performed using 11 nodes vertically in a doubly drained compressible layer ($\Delta\zeta = 0.2$), $\alpha = 0.25$, and thus a time spacing of $\Delta T = 0.01$. Further, the initial excess pore water pressure is conveniently set at 100. Because of symmetry, only the nodes from the top down to, and including, the central node need be considered. A simple hand solution for the pore pressures is shown in Table 6.1, and the isochrones are compared with those obtained from the exact Fourier series solution in Fig. 6.3.

The average degree of consolidation (Eq. 2.8) can be obtained by using a graphical integration procedure. The area under the stress surface is $2H\bar{u}_o = 200H$. The area under any subsequent isochrone may be approximated

Table 6.1 Hand Calculation of Pore Pressures using Finite Differences

T / Node	0	.01	.02	.03	.04	.05	.06	.07	.08	.09	.10
1	50	0	0	0	0	0	0	0	0	0	0
2	100	88	69	59	52	47	44	41	39	37	35
3	100	100	97	91	85	80	76	72	68	66	64
4	100	100	100	99	97	95	92	90	87	85	83
5	100	100	100	100	100	99	98	97	96	94	92
6	100	100	100	100	100	100	100	98	97	97	95
7	100	100	100	100	100	99	98	97	96	94	92

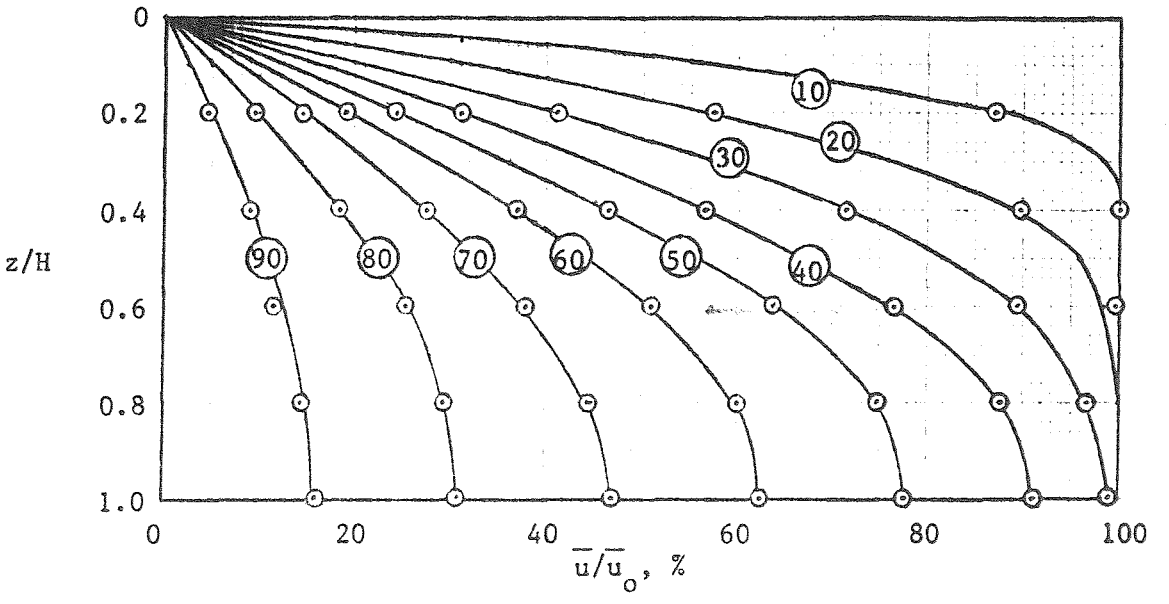

Fig. 6.3 Comparison of Pore Pressure Isochrones Calculated using Terzaghi's Theory and the Finite Difference Method. Data are shown for the upper half of a doubly drained compressible layer which is subjected to an instantaneous loading. Conditions for both analyses conform to Terzaghi's assumptions. The solid lines are the isochrones calculated using Terzaghi's theory. The hollow points are the pore pressures at nodes used in the finite difference analysis. The finite difference analysis was performed by hand, using the explicit method, and $\alpha = 1/4$. Linear interpolation was used to obtain the pore pressures at the appropriate time factors when the finite difference method was used.

using trapezoidal integration:

$$\int_0^{2H} \bar{u}dz = \tfrac{1}{2}\,\Delta\zeta\,(\bar{u}_1 + 2\bar{u}_2 + 2\bar{u}_3 + \ldots + 2\bar{u}_{n-1} + \bar{u}_n) \quad \ldots\ldots \quad (6.15)$$

or Simpson's one-third rule:

$$\int_0^{2H} \bar{u}dz = 1/3\,\Delta\zeta\,(\bar{u}_1 + 4\bar{u}_2 + 2\bar{u}_3 + 4\bar{u}_4 + \ldots + 2\bar{u}_{n-2} + 4\bar{u}_{n-1} + \bar{u}_n) \quad (6.16)$$

In Figs. 6.4 and 6.5, values of U calculated using the explicit finite difference method are compared with the values obtained using the Fourier series solution. A range in values of α and N was used, and integration was performed using Simpson's one-third rule.

The explicit method is ideal for simple hand solutions but it is cumbersome to use in computer programs where an attempt is made to model realistic conditions, and the limit of 0.5 on α is excessively restrictive and leads to very inefficient operation in certain types of problems. The restriction on α results from the fact that the two sides of Eq. 6.10 are out of synchronization in time in that the average time for the left side is $t+\frac{1}{2}\Delta t$ whereas the right side contains all terms at time t. This lack of time coordination leads to instability unless the time steps are very small, a severe restriction.

Crank-Nicholson Method

Both sides of Eq. 6.10 can be written for the time period from t to $t+\Delta t$ if the right side is replaced by the average of the pore pressures at times t and $t+\Delta t$, i.e.:

$$\frac{\bar{u}_{z,t+\Delta t} - \bar{u}_{z,t}}{\Delta t} = \tfrac{1}{2}\left[\frac{c_v}{\Delta z^2}\,(\bar{u}_{z-\Delta z,t} - 2\bar{u}_{z,t} + \bar{u}_{z+\Delta z,t}) + \frac{c_v}{z^2}\,(\bar{u}_{z-\Delta z,t+\Delta t} - 2\bar{u}_{z,t+\Delta t} - \bar{u}_{z+\Delta z,t+\Delta t})\right] \quad \ldots\ldots\ldots \quad (6.17)$$

It is convenient to re-introduce α and to factor Eq. 6.17 to place all

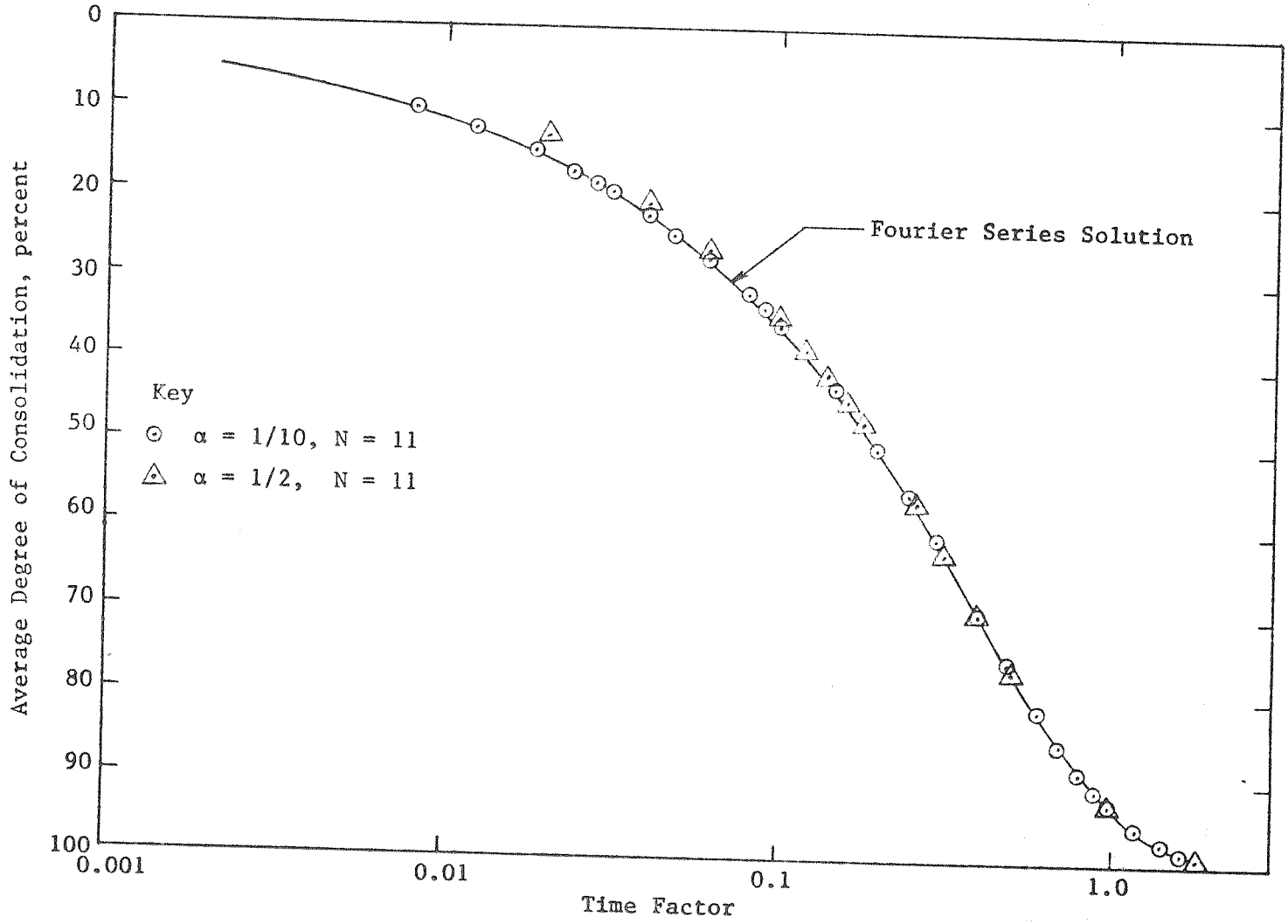

Fig. 6.4 Comparison of the Finite Difference T-U Relationship with that Obtained Using a Fourier Series. N is the number of nodes in a height 2H.

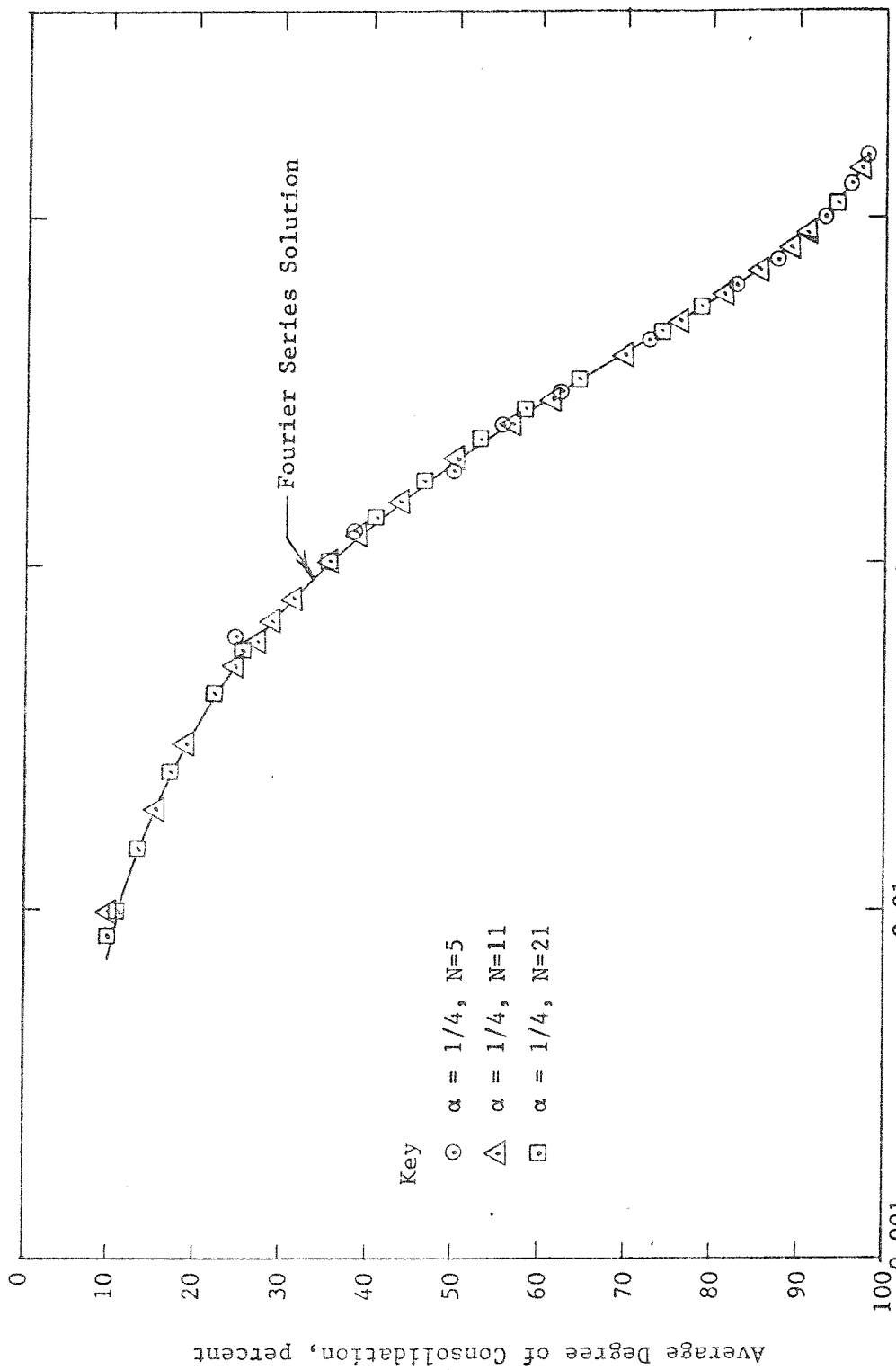

Fig. 6.5 Comparison of the Finite Difference T-U Relationship with that Obtained Using a Fourier Series. N is the number of nodes in a height 2H.

known pore pressures (those at time t) on the right side of the resulting equation and all unknown pore pressures (those at time t+Δt) on the left side. The resulting equation is:

$$-\bar{u}_{z-\Delta z,t+\Delta t} + \frac{2(1+\alpha)}{\alpha}\bar{u}_{z,t+\Delta t} - \bar{u}_{z+\Delta z,t+\Delta t} = \bar{u}_{z-\Delta z,t} + \frac{2(1-\alpha)}{\alpha}\bar{u}_{z,t} + \bar{u}_{z+\Delta z,t} \quad \ldots\ldots \quad (6.18)$$

Because the left side of Eq. 6.18 contains three unknown pore pressures, the equation cannot be solved explicitly. However, in a doubly drained layer with N nodes, there are N-2 unknown pore pressures and Eq. 6.18 can be written once for each interior node, i.e., N-2 times. Thus the unknown pore pressures are found by solution of N-2 simultaneous equations. At an impervious boundary an imaginary node is created outside the boundary with the same pore pressure as the first node inside the layer and Eq. 6.18 is written for the boundary node, i.e., at the upper impervious boundary set $\bar{u}_{z-\Delta z} = \bar{u}_{z+\Delta z}$ at all times and at a lower impervious boundary set $\bar{u}_{z+\Delta z} = \bar{u}_{z-\Delta z}$.

Because both sides of Eq. 6.18 are symmetrical with respect to both depth and time, the solution is inherently stable and values of α well in excess of 0.5 may be used. However, it is found that oscillatory solutions are obtained if α is large immediately after application of a step loading. In particular, the pore pressure at the first node inside a drainage boundary oscillates between positive and negative values for a series of iterations after a step loading. Such oscillations can be reduced to negligible proportions by using a small value of α immediately after loading but then increasing it gradually.

COMPUTER PROGRAM FD31

Further discussion of the use of finite difference methods for the solution of realistic problems is facilitated if a particular computer program is used. The program is called FD31. A list of all variables used in the program is included in Appendix A. The flow diagrams for all

subroutines are included in Appendix B and the program itself is listed in Appendix C. A user's guide for FD31 is presented in Appendix D, and example problems, including input and output, are solved in Appendix E.

In the program it is convenient to use I and J to denote depth and time nodes so Eq. 6.18 becomes:

$$-\bar{u}_{i-1,j+1} + C_L\bar{u}_{i,j+1} - \bar{u}_{i+1,j+1} = \bar{u}_{i-1,j} + C_R\bar{u}_{i,j} + \bar{u}_{i+1,j} \quad . \quad . \quad . \quad . \quad (6.19)$$

where:

$$C_L = 2(1+\alpha)/\alpha \quad . \quad . \quad . \quad . \quad . \quad . \quad . \quad . \quad . \quad . \quad . \quad . \quad . \quad . \quad . \quad (6.20)$$

$$C_R = 2(1-\alpha)/\alpha \quad . \quad . \quad . \quad . \quad . \quad . \quad . \quad . \quad . \quad . \quad . \quad . \quad . \quad . \quad . \quad (6.21)$$

$$\alpha = c_v\Delta t/(\Delta z)^2 \quad . \quad . \quad . \quad . \quad . \quad . \quad . \quad . \quad . \quad . \quad . \quad . \quad . \quad . \quad . \quad (6.22)$$

It is convenient to organize this section in terms of the assumptions made in Terzaghi's basic theory. The results of finite difference analyses will be compared with the exact Fourier series solution for Terzaghi's problem first, to show the accuracy of the program in that particular case, and then to generalize on the assumptions of the theory one by one. The capabilities of this program will thus be demonstrated in an orderly progressive manner. The details of the actual algorithm itself will be discussed subsequently.

Comparison with Terzaghi's Theory

In the context of this one section, the term "Terzaghi's Theory" means the theory that fits the assumptions listed at the beginning of Chapter 2.

Once a general method of analysis is adopted it is no longer convenient to use time factor because of the fact that variations occur in both c_v and H with time. Thus, all plots will be presented using real time. On the other hand, it is convenient to divide values of settlement by the ultimate settlement and call this ratio the average degree of consolidation, U (Eq. 2.10).

In the first test problem, the soil profile consists of one foot of sand over ten feet of clay. The water table is one hundred feet above the ground surface (so that all natural soil and fill are submerged throughout settlement). Consolidation is caused by the instantaneous application of twenty feet of fill at time zero. All soils are assigned submerged unit

weights of 50 pcf. For the clay, the void ratio is assigned a value of 2.0000 at mid-depth, of $a_v = 2.50 \times 10^{-5}$ sq.ft./lb. (this low value is used to ensure small strains and make a direct comparison with Terzaghi's theory possible), and $c_v = 0.05$ sq.ft./day.

The theoretical ultimate settlement of the clay is:

$$S = \frac{\Delta e}{1+e_o} H_o = a_v \Delta\bar{\sigma} H_o/(1+e_o) = (2.5\times10^{-5})(20\times50.0)(10)/(1+2.000)$$

$$= 0.08333 \text{ feet.}$$

The U-t curve is then calculated following standard procedures (t=500T days).

The finite difference U-t curves were obtained using a range in values of number of nodes in the clay layer (NZ) as shown in Fig. 6.6. The ultimate settlements calculated using the program were 0.08333 feet. The finite difference U-t curve is essentially exact for large times but diverges from the correct solution at small times by an amount that increases as the number of nodes decreases. The explanation for this divergence is as follows: The program does not integrate pore pressures to obtain average degrees of consolidation (Eq. 2.8) but for this particular problem the method of solution is equivalent to such an integration using the trapezoidal method. When trapezoidal integration is used and the pore pressure at a drainage boundary is specified to be zero, then there is an instantaneous dissipation of pore pressures as shown in Fig. 6.7 and the average degree of consolidation at time zero is given by:

$$U_o = 100/(NZ-1) \quad \ldots\ldots\ldots\ldots\ldots\ldots \quad (6.23)$$

where NZ is here taken as the number of nodes in a doubly drained layer. The finite difference U-t curves is Fig. 6.6 demonstrate the validity of Eq. 6.23. Accurate solutions for very small times require the use of a rather large number of nodes, e.g., 101, but such a close spacing of nodes leads to uneconomical running times (see later discussion) because it also reduces the time steps when a limit is put on α:

$$\Delta t = (\Delta z)^2/c_v\alpha \quad \ldots\ldots\ldots\ldots\ldots\ldots \quad (6.24)$$

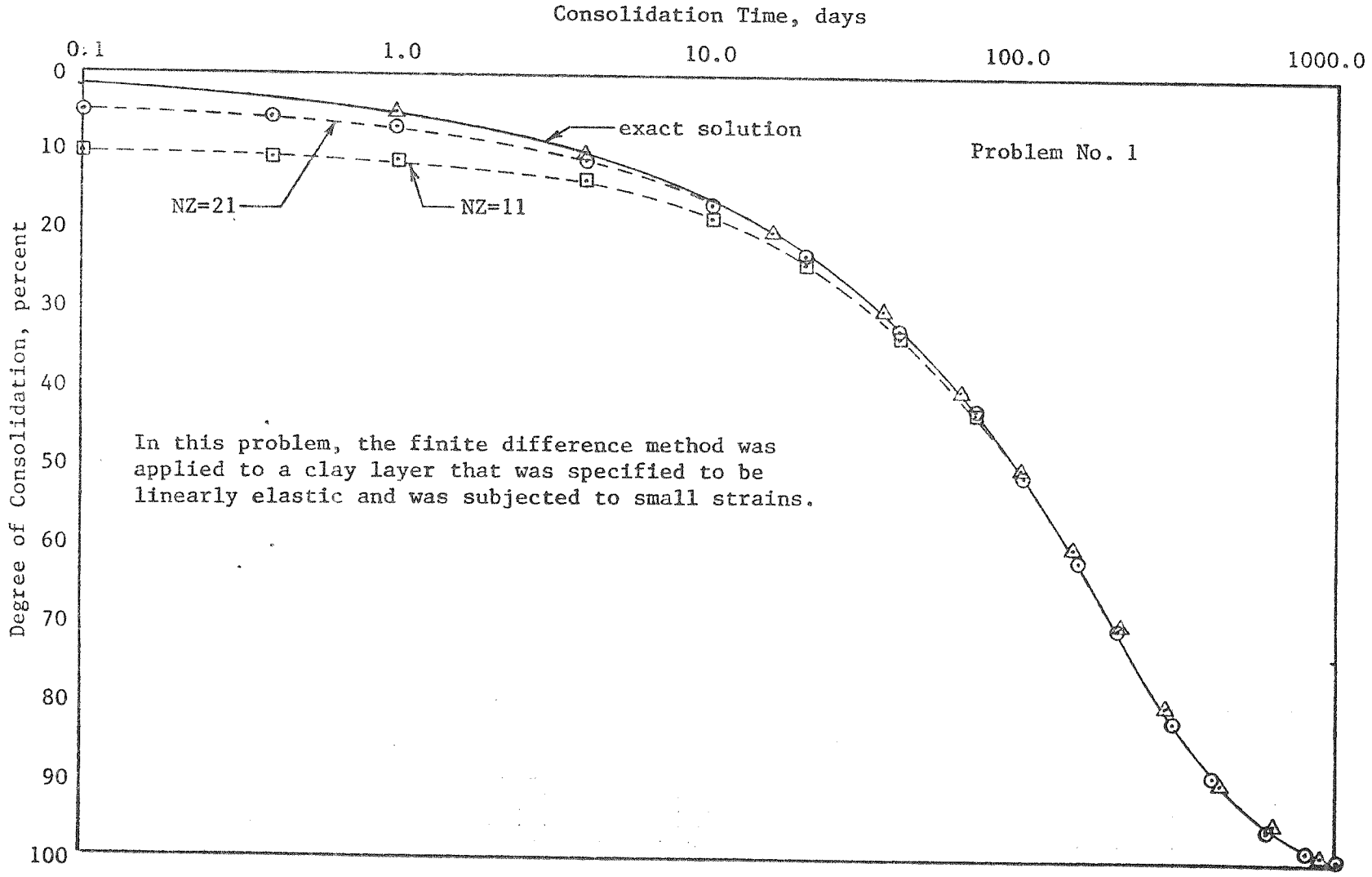

Fig. 6.6 Comparison of Finite Difference and Exact Solutions for a Case of a Step Load Applied at Time Zero

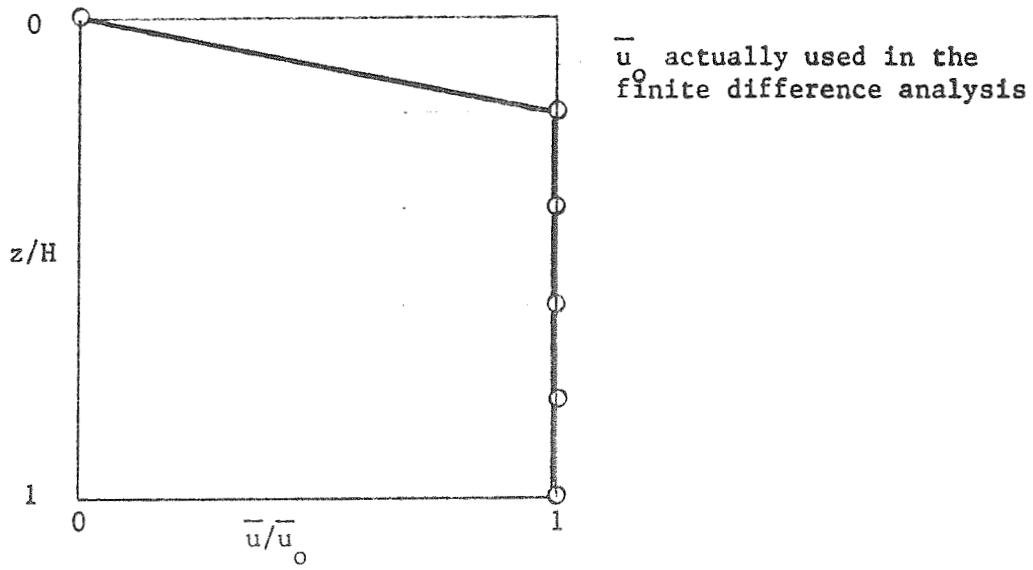

Fig. 6.7 Distribution of Initial Excess Pore Pressures at the Instant of a Step Loading

The program could be modified to operate with more nodes at the beginning and fewer later but it complicates the program unnecessary. The fact is that embankments are not constructed instantly but rather over a period of time; thus the relevant comparisons will be with exact solutions for time-dependent loads.

Time Dependent Loading

The most convenient way of taking into account time dependent loading in a finite difference program, and the way followed in FD31, is to replace the actual load-time curve with a series of step (instantaneous) loads but to make the steps sufficiently small so that the presumed load-time curve is followed with reasonable accuracy. Fill is actually applied in a series of small steps corresponding to 6"-12" of soil per lift. The time steps could be set to correspond to actual loading steps but such a level of refinement is unnecessary. In the program, the magnitude of the next time step, Δt, is calculated by methods to be discussed subsequently. The increase in applied stress that will occur during this time step, if any, is calculated and the load is applied instantly at the beginning of the step as a load Δq.

In FD31 it is assumed that the applied stress comes from an embankment (fill). If the stress comes from some other type of structure, the actual stress can easily be converted into an equivalent height of fill for purposes of analysis. The thickness of fill is specified by defining elevations of the top of the fill, E_f, at the beginning and ending of each stage of construction, and at one final point, as shown in Fig. 6.8. In the program the elevation of the top of the fill relative to a datum at the original ground surface is EFL(JL) where JL is the subscript indicating a point on the loading curve. The times corresponding to values of EFL(JL) are denoted by TL(JL). The final value of JL, denoted by JLFIN, must be at some large time because calculations stop as soon as the calculation time reaches TL(JLFIN).

It is also necessary to tell the program when construction begins and ends. Times at the beginning and ending of a construction stage (Fig. 6.8) are denoted as TFCBEG(JF) and TFCEND(JF), respectively (read

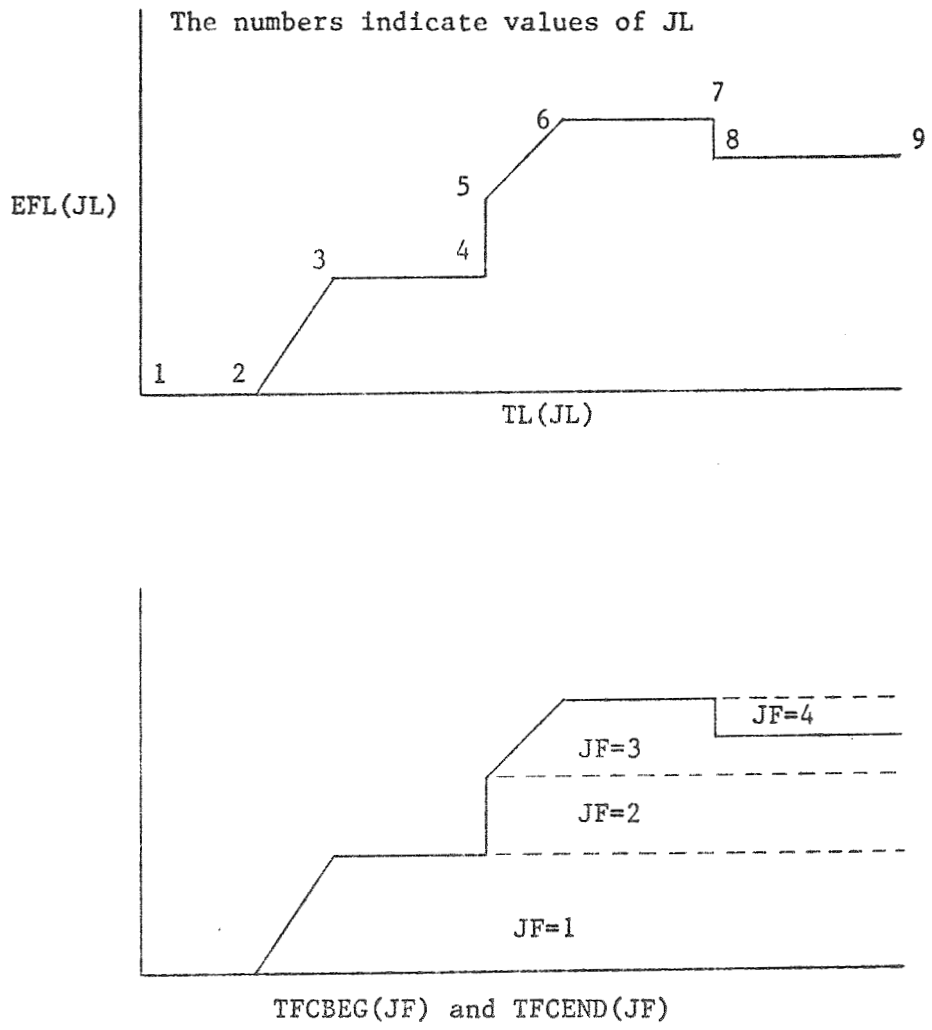

Fig. 6.8 Means used to Specify Loading Times and Fill Elevations at the End of Construction

TFCBEG as time fill construction begins and TFCEND as time fill construction ends). The total unit weight of fill during any one loading or unloading stage is GF(JF).

The time at the beginning of a time step is T in the program, and the final time is TC (read as time of calculation), and the time step is DT (read delta time). The user specifies the times for which output of data is desired as TO(JO). In chosing a time step, the program starts at the time T and attempts to jump directly to the smaller of the next TL(JL) point, or the next TO(JO). The resulting value of DT is then used to calculate the value of α for each sublayer of soil, where a sublayer is defined to be the zone of soil between any two adjacent nodes. The sublayers are indexed with IN so A(IN) denotes the value of α for the IN-th sublayer. The largest value of A(IN) in the system of layers is denoted as ALPMAX.

The upper limit on ALPMAX is termed ALPLIM. If ALPMAX exceeds ALPLIM, then the time step DT is reduced to a smaller time step (here termed DT* but just termed DT in FD31) according to:

$$DT^* = (DT)(ALPLIM)/(ALPMAX) \quad . \quad . \quad . \quad . \quad . \quad . \quad . \quad . \quad . \quad . \quad (6.25)$$

If the time step DT is during a period of loading, i.e., between TFCBEG(JF) and TFCEND(JF), then ALPLIM is set equal to an input value ALMX2. The value of ALPLIM at TL(JLFIN) is an input value ALMX3 and during the final non-construction period, which is from TL(JLFIN-1) to TL(JLFIN), ALPLIM increases linearly from ALMX2 to ALMX3. This method of limiting A(IN) has proved both effective and economical.

If the user desires to limit the time steps during a loading period directly, then a series of closely spaced values of TO(JO) are used and the program is instructed not to output detailed data at these times (otherwise a massive amount of paper is generated).

Generally, the user would like for the program to continue operating until all excess pore pressures have dissipated to suitably low values. This condition can be ensured by specifying a suitably large value for the final output time, TO(JOFIN) but then the program may waste a significant amount of computer time working with zero pore pressures because TO(JOFIN) would generally be a time well past the point where pore pressures have dissipated. To avoid this inefficiency but still ensure final dissipation

of pore pressures, the user inputs a value PPLIM (read as pore pressure limit). As soon as the absolute value of the pore pressure, $\bar{u}$, at every node is smaller than PPLIM, the program automatically terminates but the check against PPLIM is made only for values of TC greater than TL(JLFIN-1).

The accuracy of the program for a simple case will be demonstrated. The same soil profile will be used as for Fig. 6.6 except this time a single ramp loading is used with a construction time of 20 days. The pertinent controls were ALMX1=0.5, ALMX2=0.5, and ALMX3=50. The finite difference solution (Eq. 6.19) and the exact solution (Eqs. 3.8 and 3.11) are compared in Fig. 6.9. Clearly, use of just 21 nodes leads to a solution with an accuracy greater than required for practical work and the problem of inaccuracies immediately after a step load disappears.

Because the program traces any desired loading curve, it is essentially as simple to run a problem with a complicated loading diagram as for a simple diagram. Thus the artificial use of instantaneous loadings can be discontinued.

Layered Systems

In the finite difference method of analysis it is essentially as simple to analyze a layered system as a homogeneous one. The only difference is that the equation for nodes at interfaces differs slightly from that for nodes within a layer. Two conditions must be satisfied for interfacial nodes. The pore pressure must be the same in the two layers adjacent to the node and the flow out from one layer must equal the flow into the other layer. The continuity equation at an interface of unit area between an upper layer, denoted with the subscript v, and a lower layer, denoted with the subscript w, is:

$$\frac{k_v}{\gamma_w}\left(\frac{\partial \bar{u}}{\partial z}\right)_v = \frac{k_w}{\gamma_w}\left(\frac{\partial \bar{u}}{\partial z}\right)_w \qquad (6.26)$$

where k is the coefficient of permeability and γ_w is the unit weight of water. Averaged first central differences (Eq. 6.7) are used for the two derivatives to obtain:

$$k_v\left(\frac{\bar{u}_{i+1} - \bar{u}_{i-1}}{2\Delta z}\right)_v = k_w\left(\frac{\bar{u}_{i+1} - \bar{u}_{i-1}}{2\Delta z}\right)_w \qquad (6.27)$$

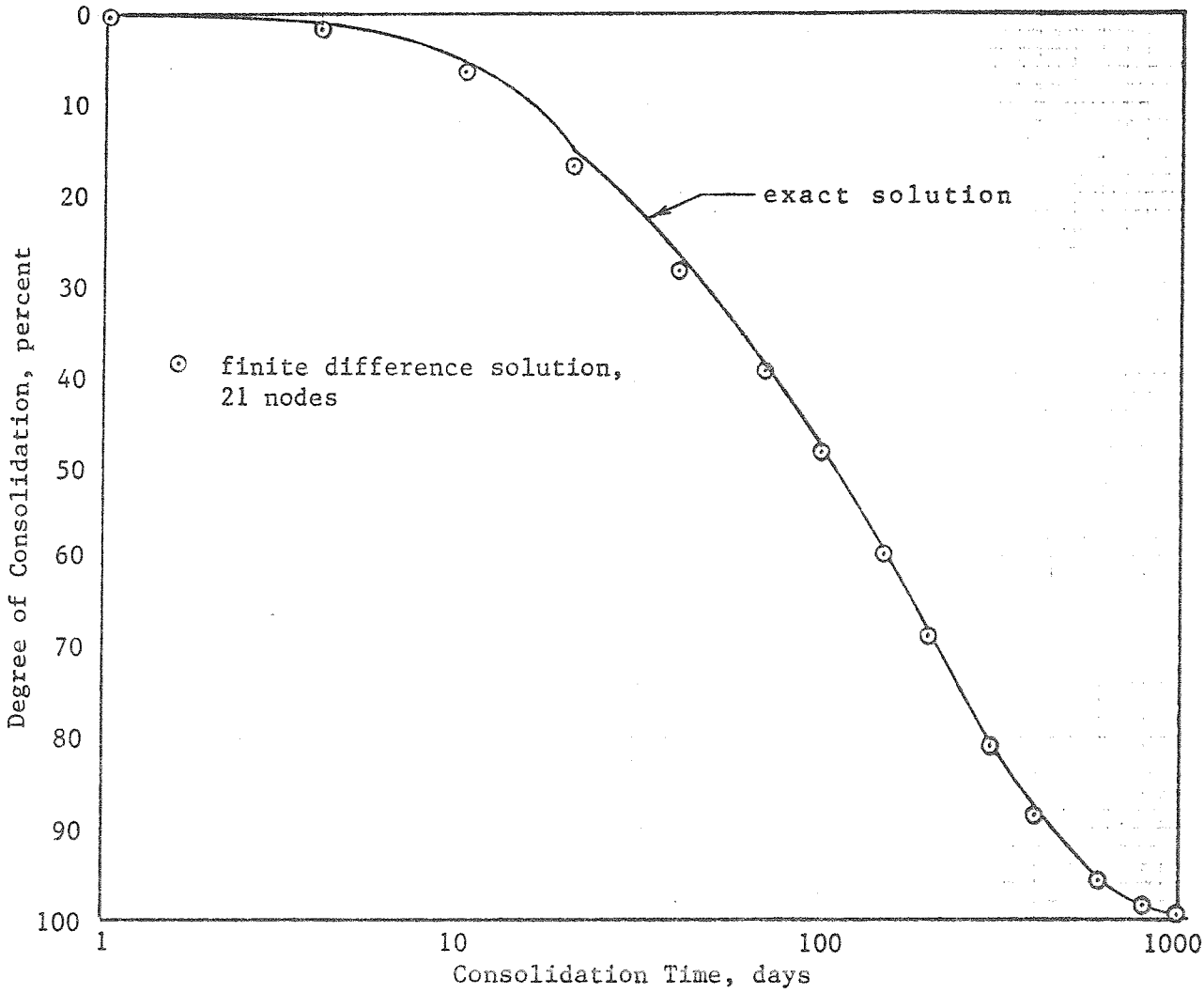

Fig. 6.9 Comparison of a Finite Difference Solution and an Exact Solution for the Case of a Single Ramp Load on a Doubly Drained Compressible Layer with Constant Properties and Subject to Small Strains

However, the node spacings will not be the same in layers v and w, nor will the properties be the same, so the pore pressures $(\bar{u}_{i+1})_v$ and $(\bar{u}_{i-1})_w$ are imaginary pore pressures. To make their imaginary nature clear in equations, $(\bar{u}_{i+1})_v$ will be replaced by v_{i+1} and $(\bar{u}_{i-1})_w$ by w_{i-1}. It is convenient to rewrite Eq. 6.27 as:

$$v_{i+1} - \bar{u}_{i-1} = \gamma(\bar{u}_{i+1} - w_{i-1}) \quad \ldots\ldots\ldots\ldots \quad (6.28)$$

where:

$$\gamma = k_w \Delta z_v / k_v \Delta z_w \quad \ldots\ldots\ldots\ldots \quad (6.29)$$

Equation 6.28 was written without a time subscript because it applies at any time. It may be written at time j and time j+1, thus introducing two equations containing four imaginary pore pressures, $v_{i+1,j}$, $v_{i+1,j+1}$, $w_{i-1,j}$, and $w_{i-1,j+1}$. Equation 6.29 is then written twice, once for the v layer considered continuous and once for the w layer continuous. A total of four equations now exist with four imaginary pore pressures. The imaginary pore pressures are eliminated to obtain the final equation:

$$-\bar{u}_{i-1,j+1} + \phi_L \bar{u}_{i,j+1} - \gamma \bar{u}_{i+1,j+1} = \bar{u}_{i-1,j} + \phi_R \bar{u}_{i,j} + \gamma \bar{u}_{i+1,j} \quad \ldots \quad (6.30)$$

where:

$$\phi_L = \frac{1 + \alpha_v}{\alpha_v} + \gamma \frac{1 + \alpha_w}{\alpha} \quad \ldots\ldots\ldots\ldots \quad (6.31)$$

$$\phi_R = \frac{1 - \alpha_v}{\alpha_v} + \gamma \frac{1 - \alpha_w}{\alpha_w} \quad \ldots\ldots\ldots\ldots \quad (6.32)$$

In a layered system, Eq. 6.19 may be used for interior nodes and Eq. 6.30 for nodes at interfaces.

To demonstrate the use of the program, analyses were performed for a two-layer system. The layers had the properties shown below:

Layer No.	e_o	c_v ft^2/day	a_v ft^2/lb	k ft/day	γ' pcf
1	2.00	0.05	0.000025	0.000026	50
2	2.00	0.25	0.000025	0.000013	50

The values of a_v were selected to ensure that strains would be small. Consolidation was induced by applying a step load of 500 psf at time zero. The finite difference analysis is compared with Gray's solution (Eqs. 3.24-3.32) for three cases as shown below:

Case 1: both boundaries freely draining

Case 2: single drainage, layer 1 adjacent to the impervious boundary

Case 3: single drainage, layer 2 adjacent to the impervious boundary

The curves of average degree of consolidation vs. time (Fig. 6.10) indicate the accuracy of the finite difference method in a two layer system.

Large and Non-Uniform Strains

The assumption of small strains occurs in the classical method of analysis when the drainage distance, H, is assumed constant during consolidation. The resulting errors are negligible for problems of building settlement where only small strains can be tolerated but for embankments, and occasionally other structures like tanks, on soft clays and peat the error may become large. For example, Weber (1969) reported a case where H decreased by nearly 80% during consolidation.

Several attempts have been made to solve one-dimensional consolidation problems involving large strains (Gibson, England, and Hussey, 1967; Mesri and Rokhsar, 1974) but such solutions are mathematically complicated and involve the imposition of severe restrictions on other soil properties so the solutions lack the generality to be generally useful.

Large and non-uniform strains are easily taken into account in the program FD31 using a new method. At the beginning of an analysis, nodes are spaced uniformly throughout each homogeneous layer of soil. The spacing will typically differ from one such layer to another, however. The soil between adjacent nodes is now considered to constitute a new layer, termed a sublayer, so that every interior node is now located at an interface and dissipation of pore pressures is controlled by the same equation, thus simplifying the equation.

An "internode" is established at the center of each sublayer. In the analysis, pore pressures and effective stresses are first evaluated at the nodes. Then the effective stresses are found at the internodes by averaging.

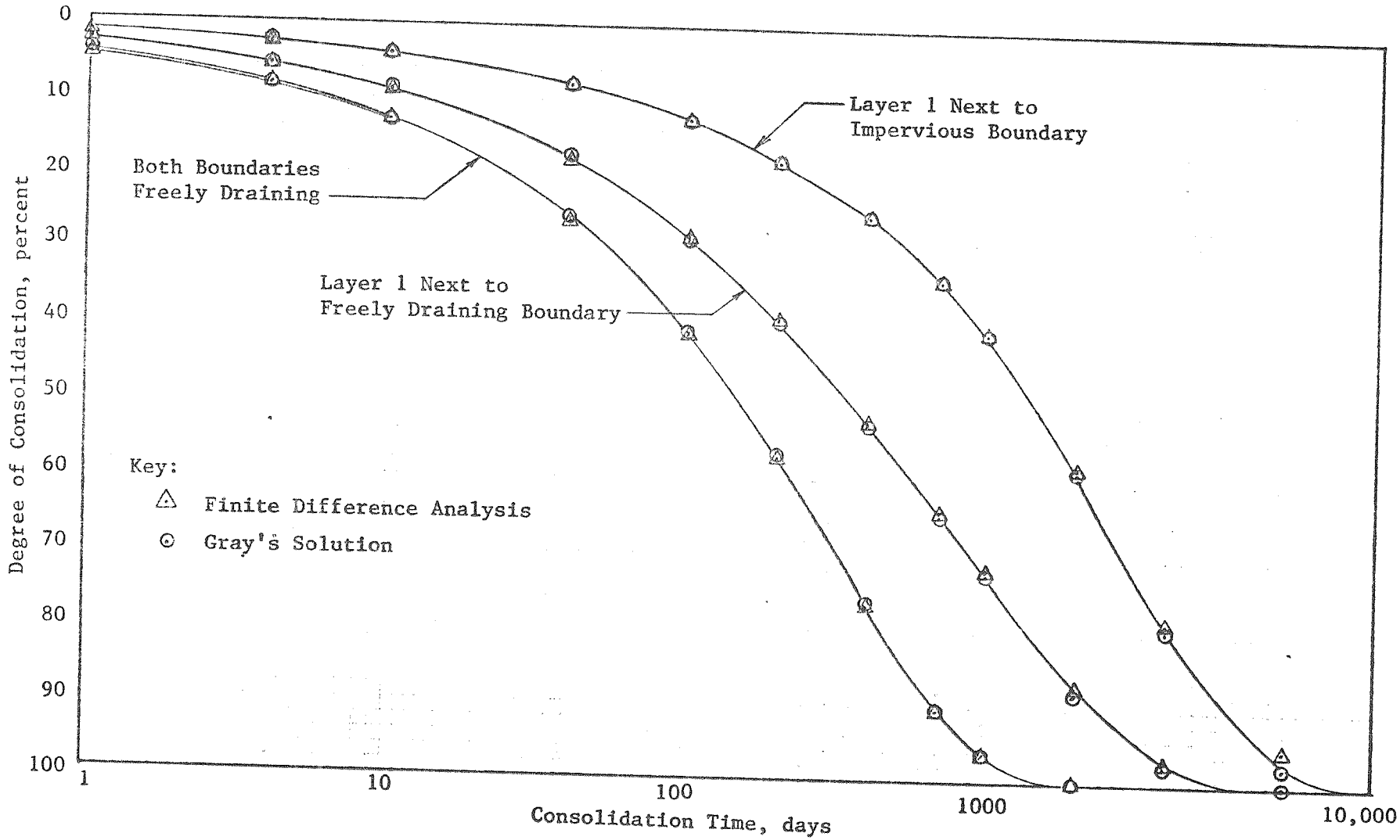

Fig. 6.10 Comparison of Theoretical Settlement Curves for Two Layer Systems

The internodal effective stress is used to find the void ratio or strain in the sublayer, which is then used to calculate the compression of the sublayer and thus the new thickness of Δz. These values of Δz are summed to obtain the surface settlement and are also used as the node spacings for the next time step. The result of using sublayers is a reduction in the length of the computer program and an automatic adjustment for both large and non-uniform strains.

To demonstrate the effects of large and non-uniform strains, analyses were performed for a highly compressible soil subject to instantly applied loads that would cause ultimate settlements of 1%, 10%, 50%, and 80% of the original thickness of the layer. The time-settlement curves calculated using finite differences (symbols) are compared with the theoretical curve calculated using Terzaghi's theory (solid curve) in Fig. 6.11. The finite difference and Fourier series solutions compare well for the case of small strains but significant errors develop for large strains. It should be emphasized that the finite difference solutions in Fig. 6.11 were obtained assuming the soil to be linearly elastic and to have a constant coefficient of consolidation.

Non-Linear Stress-Strain Curves

If the derivation of Taylor (1948) is followed, the assumption of a linear $e - \bar{\sigma}$ relationship is first required in the derivation of Eq. 2.10 where it becomes necessary to assume a constant coefficient of compressibility. Soils are not linearly elastic but the error resulting from such an assumption is generally ignored. One dimensional consolidation theories containing generalizations of this assumption have been published (Davis and Raymond, 1965; Gibson, England and Hussey, 1967; Mesri and Rokhsar, 1974) but complete generalization is feasible only for numerical methods of analysis.

In the finite-difference method of analysis, a non-linear stress-void ratio (or strain) curve is defined for each layer at a series of selected points as shown in Fig. 6.12 where E denotes void ratio or strain, and P effective stress. The calculated effective stress in each sublayer is used with the stress-strain curve of the layer to trace the proper stress-strain curve during consolidation.

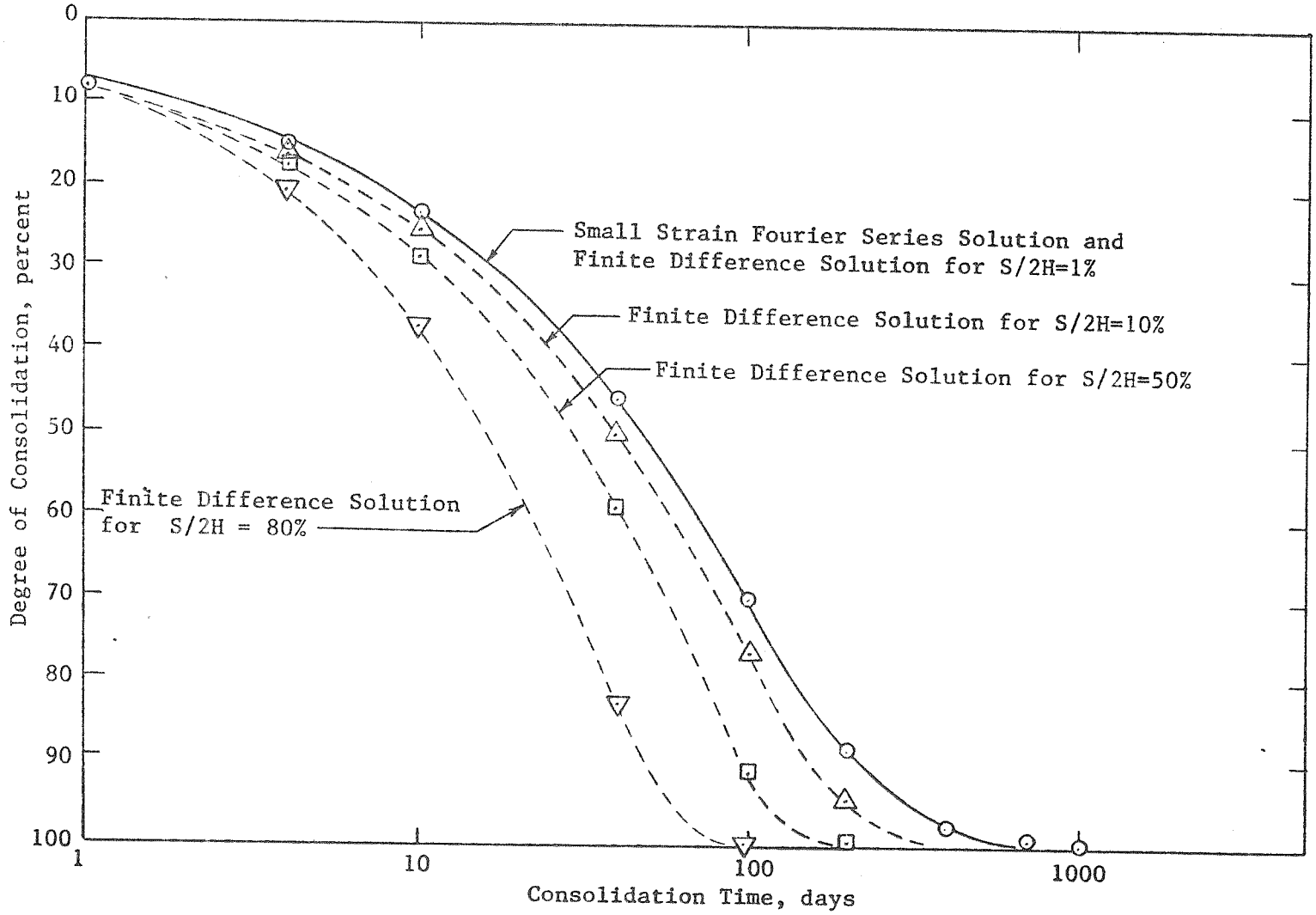

Fig. 6.11 Effects of Large Strains on the Time Rates of Consolidation

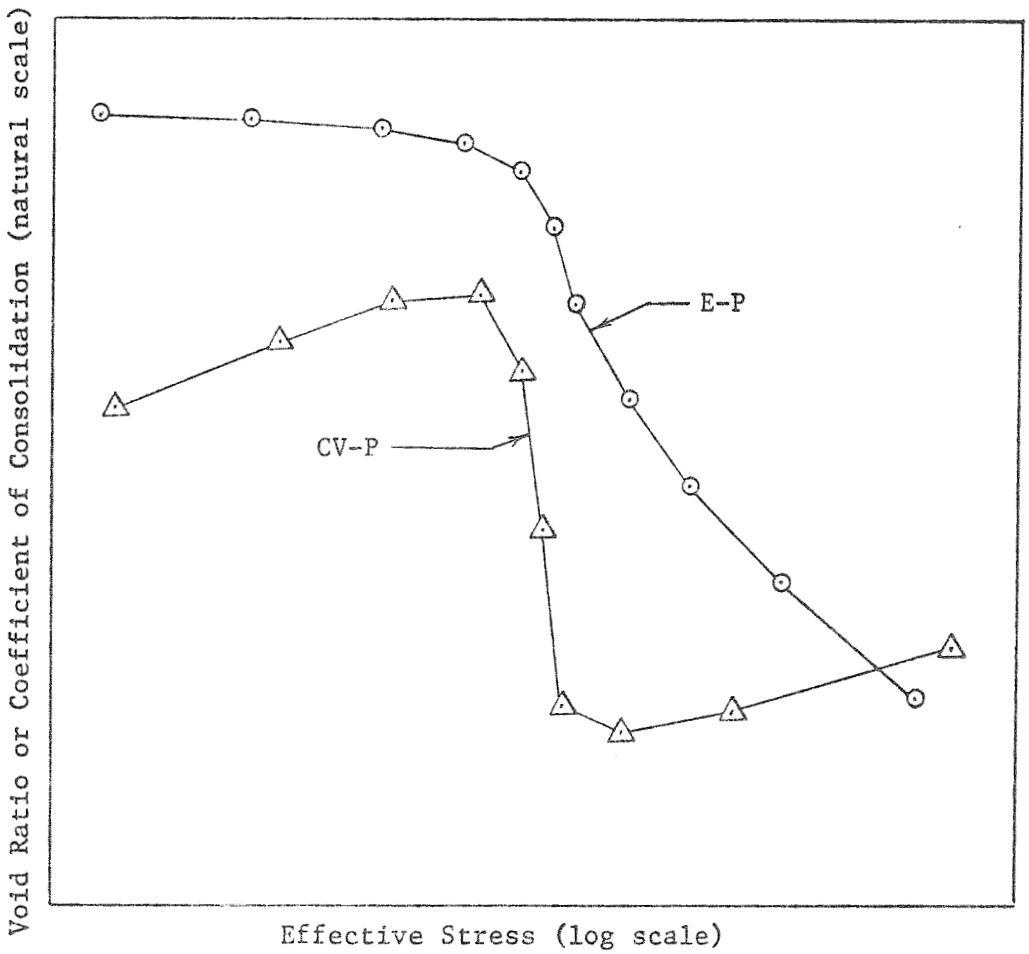

Fig. 6.12 Input Curves of Void Ratio and Coefficient of Consolidation for use in the Finite Difference Program

To demonstrate the possible magnitudes of the effects of non-linearities, a problem was selected wherein a constant stress of 5000 psf was applied to 5 ft of clay having double drainage, an average initial effective stress of 2800 psf, and c_v = 0.05 sq.ft./day. Analyses were performed using the three compression curves shown in Fig. 6.13, i.e., Case 1 with a constant coefficient of compressibility, a_v, Case 2 with a constant compression index C_c, and Case 3 for an overconsolidated clay with a maximum previous consolidation pressure of 6000 psf. The time-settlement curves calculated using finite differences, Fig. 6.13, indicate significantly retarded rates of settlement for the overconsolidated clay. In the case of a real soil the existence of a higher coefficient of consolidation for the overconsolidated clay during the reloading stage would reduce the delay indicated in Fig. 6.13.

Preloading of compressible foundation clays is often accelerated in the field by applying surcharge fills that are removed after some predetermined degree of consolidation has occurred. Unloading frequently occurs at such a time that excess pore pressure exist in the middle of the layer under the reduced load. Thus part of the layer will undergo virgin compression while the remaining portions are rebounding along a much flatter swelling curve. Classical theory cannot handle this condition and it is difficult to apply judgment to properly predict field behavior (Johnson, 1970, discusses the practical problems that can arise from this situation).

In the finite difference method of analysis it is a simple matter to allow for swelling. It is sufficiently accurate to assume that the swelling curve is linear on an e-log $\bar{\sigma}$ plot with a slope C_r. When unloading occurs, all excess pore pressures are suitably reduced and the analysis continues as before. If the effective stress at any internode decreases, the maximum effective stress and associated void ratio are stored in memory and the new void ratio at each internode is calculated using a constant swelling index and a curve that is unique to that particular internode (sublayer).

The soil profile selected to demonstrate the effects of unloading consists of one foot of freely draining sand (γ' = 70 pcf) over 20 ft of clay (γ' = 40 pcf) over additional sand, with the water table at the ground surface. The clay has c_v = 0.05 sq. ft./day and a compression curve defined by the points (e, $\bar{\sigma}$) = (2.520, 1 psf), (0.92, 8001 psf) with a constant compression index. A ramp loading of 1400 psf was applied during thirty days. Half of this load was removed at the end of various times

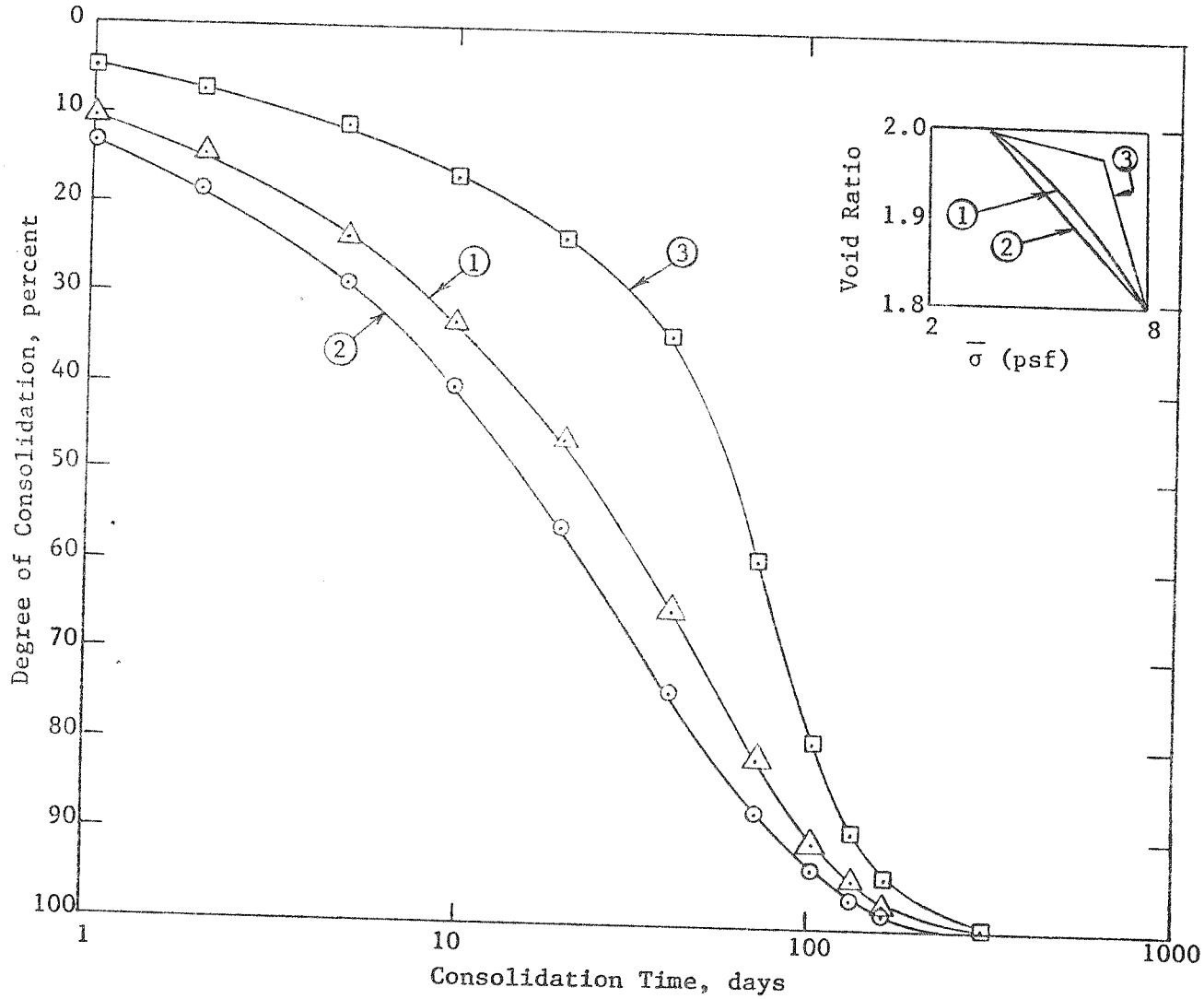

Fig. 6.13 Influence of Non-Linearity in the Stress-Strain Curve on the Computed Time-Settlement Curves when the Coefficient of Consolidation is Constant

between 30 days and 1000 days. The rebound slope was set at 20% of C_c and the time-settlement curves shown in Fig. 6.14 were calculated. The insert in Fig. 6.14 shows the effect of choosing different slopes of rebound curves.

Submergence-Settlement Correction

In a typical hand analysis of a problem involving a partially immersed fill, a submergence correction is applied at once and the applied load is assumed not to vary thereafter. In cases where large settlements are expected a trial-and-error analysis may be used to account for the effects of settlement-induced submergence of fill but the correction applies only to the final settlement, not to the time rate of settlement, and ignores such a problem as the rapid consolidation of soil near drainage boundaries under the originally applied stresses and then the rebound of this soil as the stresses are reduced by settlement-induced submergences of the fill.

In the finite difference analysis, corrections for submergence are made as the analysis progresses using the following method. The effective stress ($\bar{\sigma}$) at any point is given by

$$\bar{\sigma} = \sigma - u \quad \ldots\ldots\ldots\ldots\ldots\ldots \quad (6.31)$$

where σ is the total stress and u is the total pore water pressure. The total stress is given by:

$$\sigma = \sigma_{fw} + q + \sigma_{ns} \quad \ldots\ldots\ldots\ldots\ldots \quad (6.32)$$

where σ_{fw} is the total stress resulting from any free water ponded above the fill, q is the total stress resulting from fill, and σ_{ns} is the total stress resulting from the natural soil. If there is no water ponded above the surface then σ_{fw} is zero.

The total pore water pressure is given by:

$$u = u_s + \bar{u} \quad \ldots\ldots\ldots\ldots\ldots\ldots \quad (6.33)$$

where u_s and $\bar{u}$ are the static and excess pore pressures respectively. The static pore water pressure below the water table (see later discussion of

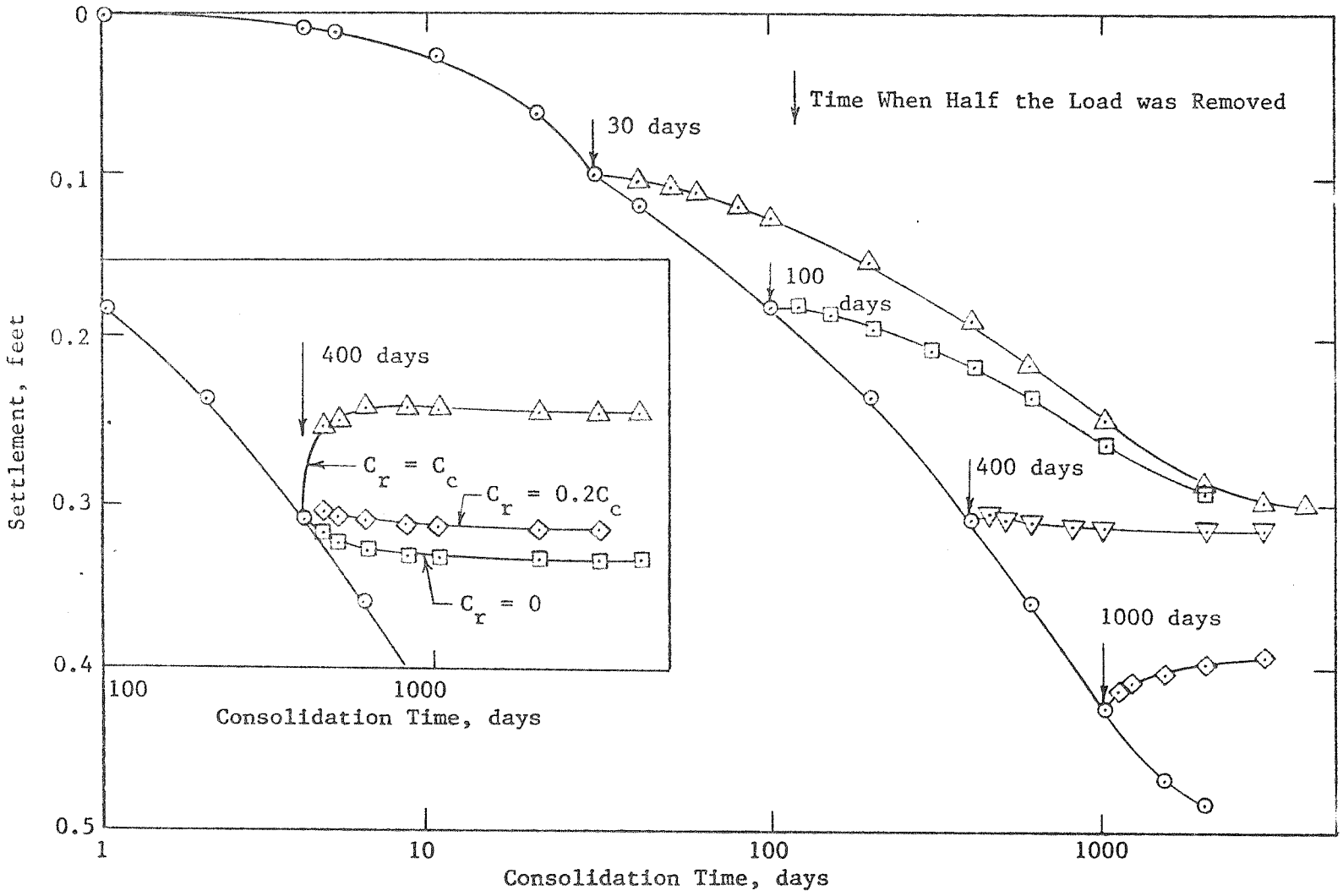

Fig. 6.14 Time-Settlement Curves with Unloading at Various Times and With Various Slopes of Swelling Curves

conditions above the water table) is defined as follows:

$$u_s \equiv (E_{wT} - E)\gamma_w \quad \ldots\ldots\ldots\ldots\ldots\ldots \quad (6.34)$$

where E_{wT} and E are the elevations of the water table and the point under consideration, respectively, relative to any arbitrary datum.

Equations 6.32 through 6.34 are inserted into Eq. 6.31 to yield;

$$\bar{\sigma} = \sigma_{fw} + q + \sigma_{ns} - (E_{wT} - E)\gamma_w \quad \ldots\ldots\ldots\ldots \quad (6.35)$$

In the analysis, the algorithm provides for a constant updating of all terms in Eq. 6.35. Note that during consolidation σ_{ns} diminishes as a result of extrusion of pore water. The "submergence correction" is thus seen as actually a correction for lost total stress.

Submergence corrections are likely to be of consequence for embankments on highly compressible soils where a large strain correction is also needed. As an example of such a problem, analyses were performed for settlement of a forty foot thick fill (γ = 132.4 pcf) applied instantly to a soil profile consisting of one foot of sand (γ = 132.4 pcf) over twenty feet of clay (γ' = 4 pcf), over sand. The water table is permanently at the elevation of the original ground surface. The coefficients of consolidation and permeability of the clay were 0.1 sq. ft./day and 0.005 ft./day, respectively. The consolidation curve of the clay passed through the following points $(e,\bar{\sigma})$ = (2.52, 1.000 psf), (0.92, 80001 psf) with a linear $e\text{-}\bar{\sigma}$ relationship. Three methods of analysis were used. In Method A (Fig. 6.15), a hand analysis was performed with no corrections for the effects of submergence, or large strain. In Method B (Fig. 6.15) a trial solution was used to calculate the final settlement with a submergence correction and the drainage distance was taken as $\frac{1}{2}(2H_o - S_u)$. In Method C (Fig. 6.15) a finite difference analysis was performed with continuous corrections for submergence, and large and non-uniform strains. The three curves are similar because of counterbalancing errors in the hand solutions. In the crudest analysis (Curve A), the excessively large ultimate settlement lowers the entire curve but use of too large a drainage distance effectively raises the curve by increasing the consolidation times. In the improved hand solution (Curve B) the final settlement is exact; the difference between curve B and the finite difference

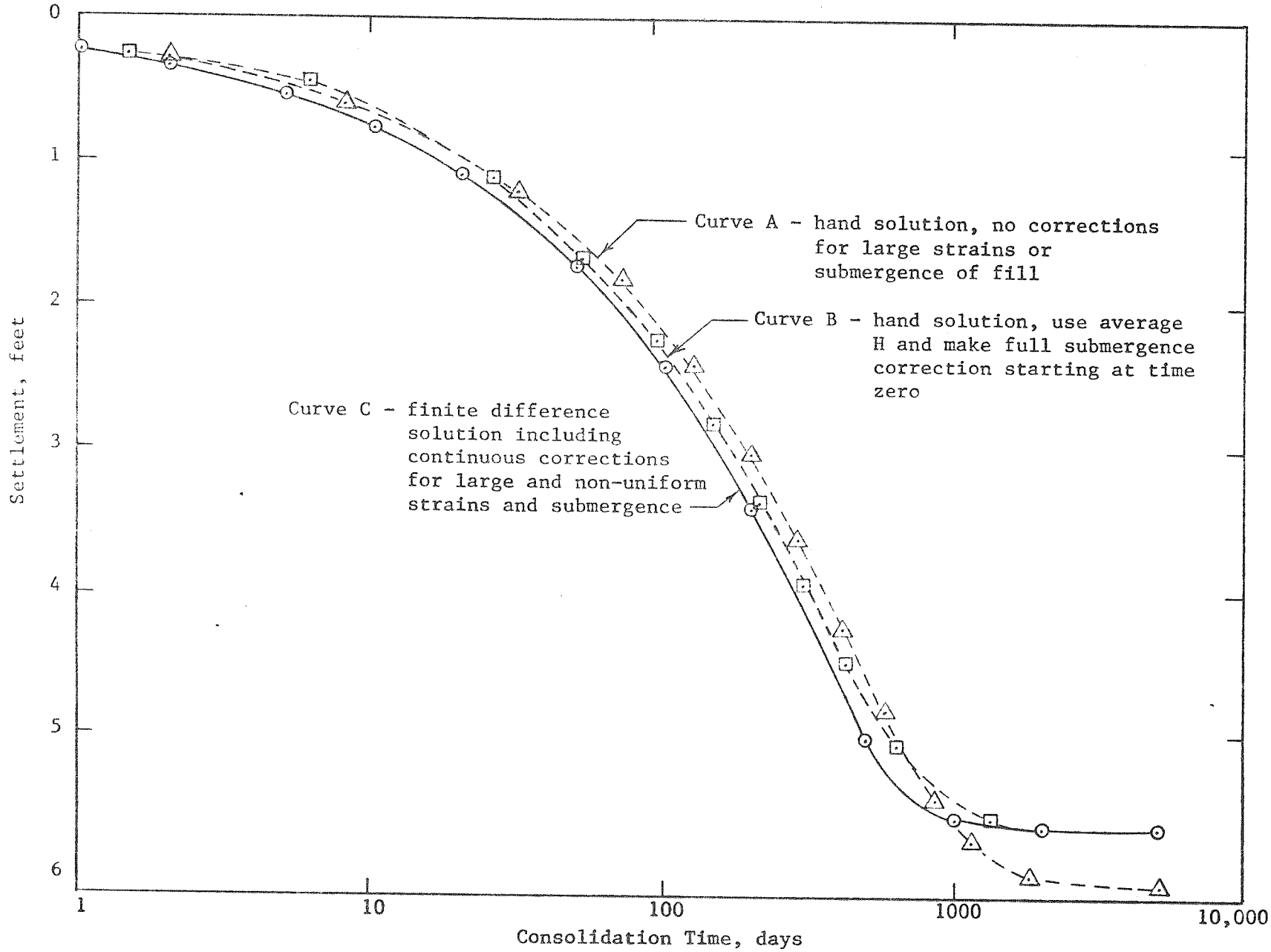

Fig. 6.15 Influence of Computational Method on Time-Settlement Curves for an Embankment on a Highly Compressible Clay with Settlement Dependent Submergence

solution results from use of a constant average H, the assumption of small strains, and the assumption of full fill submergence throughout consolidation, in the hand solution.

Effects of Changing Elevation of the Water Table

The elevation of the water table may be changed as a result of construction operations that alter surface drainage or involve either dewatering or ponding. Changes in the elevation of the water table alter the effective stresses (Eq. 6.35) and thus influence settlement. Such effects are easily included in finite difference analyses simply by updating u_s (Eqs. 6.34 and 6.35). Program FD31 provides the following options: (1) the elevation of the water table remains constant, (2) the water table rises from $E_{WT,o}$ to $E_{WT,f}$ as a result of construction operations, (3) the water table remains at the ground surface as it settles, and (4) the water table drops instantly from $E_{WT,o}$ to $E_{WT,f}$ at time zero as a result of dewatering operations.

Pore Pressures above the Water Table

The analyst may either assume zero static pore pressures above the water table or negative values equal to the distance above the water table times the unit weight of water.

Problems with Included Sand Layers

The presence of a sand layer within a clay layer poses two types of problems, one practical and one analytical.

The practical problem is to decide whether the sand layer is sufficiently extensive to provide drainage. In FD31, the analyst may specify that included sand layers are either freely draining or are sealed off.

The analytical problem results from the need for inordinately large numbers of nodes in clay layers when one or more sand layers are present, thus leading to long running times and large round-off errors. To avoid this problem, in program FD31 the presence of sand layers is taken into account in calculating total stresses but the hydraulic gradient in sand layers is considered negligible so the sand layers are provided with only top and bottom nodes and the excess pore water pressures at these nodes are identical.

The inclusion of provisions for the efficient handling of sand layers simplifies the analysis, improves the efficiency of the program greatly, and also makes it possible to take into account the presence of a surface layer of incompressible, freely draining material. The entire overburden is conveniently replaced by a single sand layer with a density chosen to give the proper stresses, and computer time is not wasted on unnecessary computations.

Variable Coefficients of Consolidation

Experience in both the laboratory (Moran, Proctor, Meuser, and Rutledge, 1958) and the field (Moran, Proctor, Meuser, and Rutledge, 1958; Olson, Daniel and Liu, 1974) show that the coefficient of consolidation may undergo substantial changes during consolidation, especially during recompression and for sensitive soils and peats. Although theories have been presented in which the coefficient of permeability varied in some analytically simple fashion (Mesri and Rokhsar, 1974; Schiffman, 1958) no usefully simple series-type solution is likely to be developed that would allow the designer to use realistic $c_v - \bar{\sigma}$ curves.

In the finite difference method of analysis it is a simple matter to account for any realistic variation of the coefficient of consolidation with effective stress for increasing loads. The coefficients of consolidation are read into computer memory at selected points on the c_v-log $\bar{\sigma}$ curve as shown in Fig. 6.12. At the end of each iteration time the effective stress at each internode is used to obtain the first approximation of the c_v for the next iteration, by linearly interpolating between points on the input c_v-log $\bar{\sigma}$ curve for that layer. The program then selects a value of Δt such that acceptably small values of α are used, performs the calculations needed to obtain all values of $\bar{\sigma}$ at the next calculation time, t_c, and obtains the new values of c_v for each layer. The fractional change in c_v at any internode, between times t and t_c, termed R, is defined as:

$$R = |c_{v,t_c} - c_{v,t}|/c_{v,t} \quad \ldots\ldots\ldots\ldots \quad (6.36)$$

where $c_{v,t}$ and c_{v,t_c} are the values of c_v at any internode at times t and t_c, respectively. The value of R is evaluated for each internode. If every value

of R is less than an input value, R_{min}, then the analysis proceeds to the next time step. On the other hand, if any value of R exceeds an input upper limit, R_{max}, then the time step is reduced from Δt to Δt^* where:

$$\Delta t^* = \Delta t(R/R_{max})0.9 \quad . . . . . \quad (6.37)$$

and calculations are begun again for the new time step. If any value of R exceeds R_{min} but no value exceeds R_{max}, then the calculations are repeated for the same time step, Δt, but the value of c_v used in each sublayer is the average of the values perviously calculated at times t and t_c.

Numerous analyses have been performed in which variable-property finite difference solutions were compared with either constant-property finite difference solutions or with classical analyses. The only general conclusion that can be drawn from such comparisons is that there is a possibility of gross error when classical analyses are used. As an example of the results obtained, the following case was analyzed. The soil consists of 14 ft of incompressible sand (γ' = 70 pcf) over 10 ft of compressible clay (γ' = 20 pcf), over sand. The water table remains at the elevation of the original ground surface. Twenty feet of fill (γ = 132.4 pcf) was placed during a construction period of ten days. The e-log $\bar{\sigma}$ and c_v-log $\bar{\sigma}$ relationships for the clay are shown in the insert of Fig. 6.16. A curve of U vs log time was calculated using the proper c_v-log $\bar{\sigma}$ relationship (Fig. 6.16). Then a constant-property analysis was performed using a c_v of 0.75 sq. ft/day, which was the average of the initial and final values (Fig. 6.16). A second constant-properties solution was obtained using a c_v of 0.35 sq. ft/day, which was the average value in the stress range where most of the compression was occurring. Note that for all solutions corrections were made for large and non-uniform strains and submergence of the fill, and all utilized the same e-log $\bar{\sigma}$ curve. Significantly different constant-properties curves result even though either seemed based on a reasonable averaging process to obtain c_v. However, neither constant-property solution yields a settlement curve of the proper shape. In the real case (variable properties), the effective stresses near drainage boundaries increase rapidly to values in excess of 200 psf where c_v is a minimum. Thus, a comparatively impervious skin formed adjacent to the drainage boundaries and retarded consolidation.

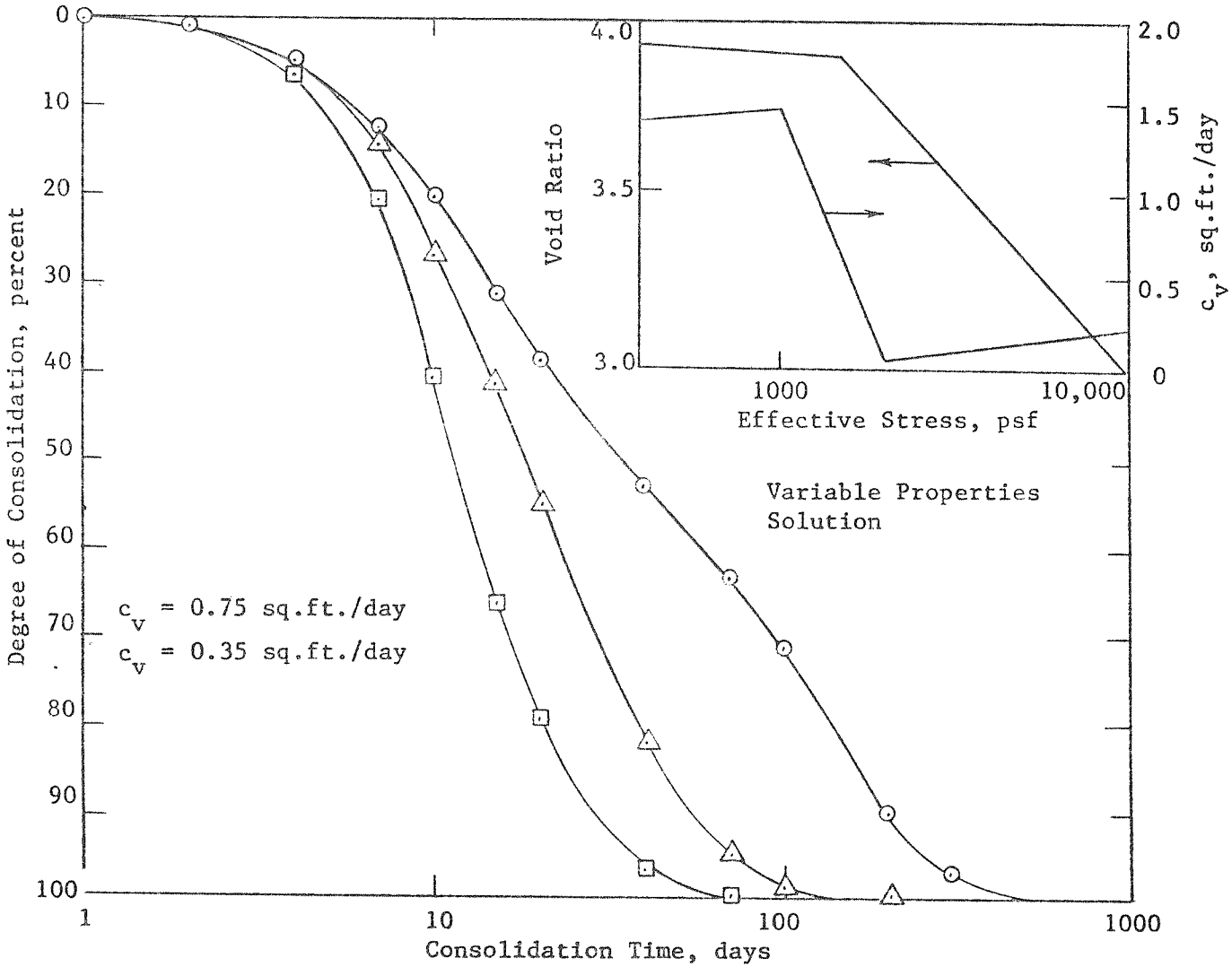

Fig. 6.16 Comparison of Constant-Property and Variable Property Solutions for the Time-Settlement Curve

CHAPTER 7

CONCLUDING REMARKS

The beginning of modern soil mechanics was at the time Terzaghi published his theory for one-dimensional consolidation. The resulting elucidation of the principle of effective stress and of the role of pore water pressures in influencing the response of soils to changed loads, led to rapid evolution in essentially all aspects of geotechnical engineering. One of the fundamental building blocks of college education in soil mechanics has been an understanding of Terzaghi's theory of consolidation. It is also a widely used tool among practicing foundation engineers.

In considering the fundamental nature of the theory and its wide application, one is struck with the curious lack of field evidence that the theory actually describes what happens on real projects. A careful study of the available literature suggests that in the case of one-dimensional problems, at least, the difficulty is not so much in the basic formulation of the theory as it is in achieving solutions under realistic conditions. Thus, field problems typically involve stratified soils subject to time dependent loading, soils are not linearly elastic, they may be subjected to large and non-uniform strains, the coefficients of permeability and compressibility vary with effective stress, and stress conditions are altered by a changing water table and settlement-dependent submergence of soil. Only when these complications are taken into account will it be possible to examine field data for evidence of the accuracy of the underlying assumptions of the theory.

Closed-form mathematical solutions are unlikely ever to describe field conditions in a generally useful way. The first problem with closed form solutions is that soil properties must be described using analytic functions so the equations can be integrated. Soil properties are not well described by simple functions. The second problem is simply that inclusion of all relevant effects results in such severe mathematical problems that a solution cannot be achieved. The third problem is that even if suitable functions were found and integrated, the resulting equations would be too cumbersome to be applied to real problems.

A comparatively simple solution can be achieved using numerical methods. Realistic properties and field conditions are fed into a computer and calculations are controlled by a relatively simple set of instructions to the machine. Each practical problem is thus solved explicitly and no attempt is made to come up with design corves or tables.

The finite difference program FD31 was written to achieve such a "solution" for one-dimensional consolidation problems. As discussed in Chapter 6, this program makes it possible to analyze many practical problems with an accuracy never before attainable. It will now be necessary to improve our methods of measurement of soil properties and our ability to determine actual field conditions so the full potential of this method can be realized.

Further developments are needed to account for multidirectional effects, for three phase systems, and for creep.

REFERENCES

Abbott, M. B. (1960), "One-Dimensional Consolidation of Multi-Layered Soils," Geotechnique, Vol. 10, pp. 151-165.

Aboshi, H., and H. Mondin (1963), "Determination of the Horizontal Coefficient of Consolidation in an Alluvial Clay," Proceedings, Fourth Australian - New Zealand Conference on Soil Mechanics and Foundation Engineering, pp. 159-164.

Aldrich, H. P. (1965), "Precompression for Support of Shallow Foundations," Journal of the Soil Mechanics and Foundations Division, ASCE, Vol. 91, SM5, pp. 471-506.

Bishop, A. W., and R. E. Gibson (1964), "The Influence of the Provisions for Boundary Drainage on Strength and Consolidation Characteristics of Soil Measured in the Traixial Apparatus," ASTM STP361, pp. 435-451.

Burn, K. N. (1969), "Settlement of a High Embankment and Overpass Structures in Ottawa," Canadian Geotechnical Journal, Vol. VI, NO. 1, pp. 33-48.

California Division of Highways (1974), "Foundation and Seismic Investigation for the Existing and Proposed State Capitol Building Sites," unpublished report, October.

Casagrande, A. and R. E. Fadum (1944), "Application of Soil Mechanics in Designing Building Foundations," Trans., ASCE, Vol. 109, pp. 383-490.

Casagrande, L, L. Firing, G. Schoof, and E. W. Turcke (1965), "Settlement of Mat Foundation on nhick Stratum of Sensitive Clay," Canadian Geotechnical Journal, Vol. II, No. 2, pp. 299-312.

Cedergren, H. R. and W. G. Weber (1962), "Subsidence of California Highways," ASTM SPT322, pp. 248-264.

Chang, Y. C. E., B. Broms, and R. B. Peck (1973), "Relationship Between the Settlement of Soft Clays and Excess Pore Pressures Due to Imposed Load," Proceedings, Eighth Int. Conf. on Soil Mech. and Foundation Engin., Moscow, Vol. 1.1, pp. 93-96.

Cooling, L. F. (1948), "Settlement Studies at Waterloo Bridge," Proceedings, Second Int. Conf. on Soil Mech. and Foundation Engin., Rotterdam, Vol. II, pp. 130-134.

Cox, Joel B. (1936), "The Alexander Dam, Soil Studies and Settlement Observations," Proceedings, INtern. Conf. on Soil Mech. & Found. Engr., Vol. 2, pp. 296-297.

Crawford, C. B. and J. G. Sutherland (1971), "The Empress Hotel, Victoria, British Columbia. Sixty-Five Years of Foundation Settlements," Canadian Geotechnical Journal, Vol. 8, No. 1, pp. 77-93.

Darragh, R. E. (1964), "Controlled Water Tests to Preload Tank Foundations," Journal of the Soil Mechanics and Foundations Division, ASCE, Vol. 90, SM5, pp. 303-329.

Davis, E. H., and G. P. Raymond (1965), "A Non-Linear Theory of Consolidation," Geotechnique, Vol. 15, No. 2, pp. 161-173.

Desai, C. S., and L. D. Johnson (1972), "Evaluation of Two Finite Element Formulations for One-Dimensional Consolidation," Computers and Structures, 2, pp. 469-486.

Desai, C. S. and L. D. Johnson (1973), "Evaluation of Some Numerical Schemes for Consolidation," International Journal for Numerical Methods in Engineering, Vol. 7, pp. 423-254.

Gibson, R. E., G. L. England, and M. J. L. Hussey (1967), "The Theory of One-Dimensional Consolidation of Saturated Clays, 1. Finite Non-Linear Consolidation of Thin Homogeneous Layers," Geotechnique, Vol. 17, pp. 261-273.

Gibson, R. E. and P. Lumb (1953), "Numerical Solution of Some Problems in the Consolidation of Clay," Proceedings, Institution of Civil Engineers, (Pt. I), Vol. 2, Part 2, p. 182.

Gibson, R. E. and A. Marsland (1960), "Pore-Water Pressure Observations in a Saturated Alluvial Deposit Beneath a Loaded Oil Tank," Pore Pressure and Suction in Soils, pp. 112-118.

Gould, T. P. (1949), "Analysis of Pore Pressure and Settlement Observations at Logan International Airport," Harvary Soil Mechanics Series No. 34, Harvard University, Cambridge, Mass.

Gray, H. (1945), "Simultaneous Consolidation of Contiguous Layers of Unlike Compressible Soils," Transactions, ASCE, Vol. 110, pp. 1327-1344.

Haefeli, R. and W. Schaad (1948), "Time Effect in Connection with Consolidation Tests," Proceedings, Sec. Intern. Conf. on Soil Mech. & Found. Engr., Vol. 3, pp. 23-29.

Hanrahan, E. T. (1964), "A Road Failure on Peat," Geotechnique, Vol. 14, No. 3, pp. 185-202.

Henkel, D. J. (1965), "Problems Associated with the Construction of the Ebute Metta Causeway over Soft Clays in Lagos, Nigeria," Proceedings, Sixth Int. Conf. on Soil Mech. & Found. Engr., Montreal, Vol. 1, pp. 74-77.

Herbert, M. F. L. and P. W. Rowe (1973), "Design and Performance of Two Coal Stacks on Soft Clay at the N.C.B. Bulk Terminal, Immingham," Geotechnique, Vol. 23, No. 2, pp. 245-261.

Holtz, R. E. and G. Lindskog (1972), "Soil Movements Below a Test Embankment," Proceedings, ASCE Specialty Conf. on Performance of Earth and Earth-Supported Structures, Vol. I, Part 1, Purdue University, pp. 273-384.

Hutchinson, J. N. (1964), "Settlements in Soft Clay Around a Pumped Excavation in Oslo," NGI Publication 58.

James, P. M. (1970), "The Behavior of a Soft Recent Sediment Under Embankment Loadings," Quarterly Journal of Engineering Geology, Vol. 3, No. 1, pp. 41-53.

Johnson, S. J. (1970), "Precompression for Improving Foundation Soils," Journal of Soil Mechanics and Foundation Engineering, ASCE, Vol. 96, No. SM1, pp. 111-144.

Jonas, E. (1964), "Subsurface Stabilization of Organic Silty Clay by Precompression," Journal of the Soil Mechanics and Foundations Division, ASCE, Vol. 90, MS5, pp. 363-376.

Justo, J. L. (1969), "Instrumentation of a New Channel in Soft Ground," Proceedings, Seventh Intern. Conf. on Soil Mech. and Found. Engr., Mexico City, Vol. 2, pp. 599-607.

Kaufman, R. I. and W. C. Sherman (1964), "Engineering Measurements for Port Allen Lock," Journal of the Soil Mechanics and Foundations Division, ASCE. Vol. 90, SM5, pp. 221-247.

Kimball, W. P. (1936), "Settlement Records of the Mississippi River Bridge at New Orleans," Proceedings, First Intern. Conf. on Soil Mech. and Found. Engr., Harvard University, Vol. I, pp. 85-98.

Kleiman, W. F. (1964), "Use of Surcharges in Highway Construction," Journal of the Soil Mechanics and Foundations Division, ASCE, Vol. 90, SM5, pp. 331-348.

Kotzias, P. C. and A. C. Stamatopoulos (1969), "Preloading for Heavy Industrial Installations," Journal of the Soil Mechanics and Foundations Division, ASCE, Vol. 95, SM6, pp. 1335-1355.

Kuessel, T. R., B. Schmidt, and D. Rafaeli (1973), "Settlemtns and Strengthening of Soft Clay Accelerated by Sand Drains," Highway Research Board Bulletin 457, pp. 18-26.

Ladd, C. C., J. J. Rixner, and D. G. Gifford (1972), "Performance of Embankments with Sand Drains on Sensitive Clay," Proceedings, ASCE Specialty Conference on Performance of Earth and Earth-Supported Structures, Purdue University, Vol. I, Part 1, pp. 211-242.

Lake, J. R. (1961), "Pore-Pressure and Settlement Measurements During Small-Scale and Laboratory Experiments to Determine the Effectiveness of Vertical Sand Drains in Peat," Conf. on Pore Pressure and Suction in Soils, London, pp. 103-107.

Lambe, T. W. (1969), "Reclaimed Land in Kawasaki City, Japan," Journal of the Soil Mechanics and Foundations Division, ASCE, Vol. 95, SM5, pp. 1181-1198.

Lindskog, G., and B. B. Broms (1970), Discussion of "On the Effectiveness of Sand Drains," Canadian Geotechnical Journal, Vol. 7, No. r, pp. 508-510.

Lo, K. Y. (1961), "Secondary Compression of Clays," Proceedings, ASCE, Vol. 87, MS4, pp. 61-88. disc. 87:SM6, 88:SM1, 88:SM4.

McAlpin, G. W. and M. N. Sinacori (1955), "Sand Drains for Embankment on Marl Foundation," Highway Research Board Bulletin 115, pp. 15-30.

Mesri, G. (1973), "Coefficient of Secondary Compression," Jour. of the Soil Mech. and Found. Div., ASCE, VOL. 99, No. SM1, pp. 123-137.

Mesri, G., and A. Rokhsar (1974), "Theory of Consolidation for Clays," Journal of the Geotechnical Engineering Division, ASCE, Vol. 100, No. GT8, pp. 889-904.

Miyahara, Y., R. Nakamura, and M. Takayama (1967), "Improved Strength of Clay Layer by Means of Sand Drain Foundation," Proceedings, Third Asian Reg. Conf. on Soil Mech. and Found. Engr., Haifa, Israel, pp. 305-307.

Moh, Z. C., E. W. Brand, and J. D. Nelson (1974), "Pore Pressures Under a Bund on Soft Fissured Clay," Proceedings, ASCE Specialty Conference on Performance of Earth and Earth-Supported Structures, Purdue Univ., Vol. I, Part 1, pp. 243-272.

Moore, L. H. and T. Grosert (1968), "An Appraisal of Sand Drain Projects Designed and Constructed by the New York Department of Transportation," New York State Department of Transportation Physical Research Report No. 5.

Moran, Proctor, Mueser, and Rutledge (1958), "Study of Deep Soil Stabilization by Vertical Sand Drains," OTS Report PB151692.

Murray, R. T. (1971), "Embankments Constructed on Soft Foundations: Settlement Study of Avonmouth," Road Research Laboratory Report LR419.

Nonveiller, E., and I. Kleiner (1969), "Calculated and Observed SEttlement of a Silo Group," Proceedings, Seventh Intér. Conf. on Soil Mech. and Found. Engr., Mexico City, Vol. 2, pp. 195-201.

Olson, R. E. (1977), "Consolidation Under Time Dependent Loading," Jour. Geot. Engr. Div., ASCE, Vol. 103, Nol GT1, pp. 55-60.

Olson, R. E., D. E. Daniel, and T. K. Liu (1974), "Finite Difference Analyses for Sand Drain Problems," Analysis and Design in Geotechnical Engineering, ASCE Vol. 1, pp. 85-110.

Olson, R. E. and C. C. Ladd (1977), "Analysis of One-Dimensional Consolidation Problems," Jour. Geotechnical Engr. Div., ASCE, (submitted).

O'Neill, D. F. (1954), "Permeability Determinations During Consolidation Testing," B.S. Thesis, M.I.T.

Ortiz, I. S. (1966), "Zumpango Test Embankment," Proceedings, ASCE Specialty Conf. on Performance of Slopes and Embankments, Univ. of California at Berkeley, pp. 221-231.

Rafaeli, D. (1972), "Design of the South Island for the Second Hampton Roads Crossing," Proceedings, ASCE Specialty Conf. on Performance of Earth and Earth-Supported Structures, Purdue Univ., Vol. I, pp. 361-378.

Richart, F. E., Jr. (1957), "A Review of Theories for Sand Drains," Journal of the Soil Mech. and Found. Div., ASCE, Vol. 83, No. SM3, Paper 1301.

Root, A. W. (1958), "California Experience in construction of Highways Across Marsh Deposits," Highway Research Board, Bulletin 173, pp. 46-64.

Samson, L., and R. Garneau (1973), "Settlement Performance of Two Embankments on Deep Compressible Soils," Canadian Geotechnical Journal, Vol. 10, No. 2, pp. 211-226.

Schiffman, R. L. (1958), "Consolidation of Soil Under Time-Dependent Loading and Varying Permeability," Proceedings, Highway Research Board, Vol. 37, pp. 384-617.

Schiffman, R. L. (1972), "The Efficient Use of Computer Resources," Applications of the Finite Element Method in Geotechnical Engineering, C.S. Desai, ed. (preprint).

Schiffman, R. L. and R. V. Whitman (1966), "ICES-SEPOL-I, A Settlement Problem Oriented Language - Systems Design," Tech. Report T66-3, Department of Civil Engineering, M.I.T.

Schiffman, R. L., R. V. Whitman, and J. C. Jordan (1970), "Settlement Problem Oriented Computer Language," Proceedings, ASCE, Journal of the Soil Mechanics and Foundations Division, ASCE, Vol. 96. No. SM2, pp. 649-669.

Schmidt, T. J., and J. P. Gould (1968), "Consolidation Properties of an Organic Clay Determined from Field Measurements," Highway Research Record, No. 243, pp. 38-48.

Scott, R. F. (1953), "Numerical Analysis of Consolidation Problems," unpublished M.S. Thesis, M.I.T., Department of Civil Engineering.

Stermac, A. G., K. Y. Lo, and A. K. Barsvary (1967), "The Performance of an Embankment on a Deep Deposit of Varved Clay," Canadian Geotechnical Journal, Vol. IV, No. 1, pp. 45-61.

Taylor, D. W. (1942), Research on Consolidation of Clays, Mass. Inst. of Tech., Serial 82, 147 pp.

Taylor, D. W. (1948), Fundamentals of Soil Mechanics, John Wiley and Sons, Inc., New York, New York.

Terzaghi, K. (1923a), "Die Berechnung der Durchlassigkeitsziffer des Tones aus dem Verlauf der Hydrodynamischen Spannungserscheinungen," Akademie der Wissenschaften in Wein. Sitzungsberichte, Mathematisch-naturwissenschaftliche Klasse. Part IIa, 132, No. 3/4, pp. 125-138.

Terzaghi, K. (1923b), "Die Beziehungen Zwischen Elastizitat und Innendruck," Akademie der Wissenschaften in Wein. Stizungsberichte. Mathematisch-naturwissenschaftliche Klasse. Part IIa, 132, pp. 105-124.

Terzaghi, K., and O. K. Frohlich (1936), Theorie der Setzung von Tonschiten, F. Deuticke, Leipzig.

Thompson, James B. and L. A. Palmer (1951), "Report of Consolidation Tests with Peat," ASTM STP No. 126, pp. 4-8.

Tsien, S. I. (1955), "Stabilization of Marsh Deposit," Highway Research Board Bulletin 115, pp. 31-43.

U.S. Army Corps of Engineers, New Orleans District (1968), "Interim Report, Field Tests of Levee Construction, Test Sections I, II, and III."

Varghese, P. C. and B. Ramanthan (1971), "Settlement of Oil Tanks near Madras (India)," Proceedings, Fourth Asia Regional Conf. on Soil Mech. and Found. Engr. Bangkok, Vol. 1, pp. 329-334.

Walker, F. H. (1966), "Willard Dam = Behavior of a Compressible Foundation," Proceedings, ASCE Specialty Conference on Stability and Performance of Slopes and Embankments, Univ. of California at Berkeley, pp 199-220.

Wallace, G. B. and W. C. Otto (1964), "Differential Settlement at Shelfridge Air Force Base, Journal of the Soil Mechanics and Foundations Division, ASCE, Vol. 90, SM5, pp. 197-220.

Webber, R. and W. C. Hill (1955), "Modification of Sand Drain Principle for Pressure Relief in Stabilizaing Embankment Foundation," Highway Research Board Bulletin 115, pp. 1-14.

Weber, W. G. (1966), "Experimental Sand Drain Fill at Napa River," Highway Research Record, No. 133, pp. 32-44.

Weber, W. G. (1968), "In-Situ Permeabilities for Determining Rates of Consolidation," Highway Research Record, No. 243, pp. 49-61.

Weber, W. G. (1969), "Performance of Embankments Constructed Over Peat," Journal of the Soil Mechanics and Foundations Division, ASCE, Vol. 95, SM1, pp. 53-76.

Wu, T. H., and R. B. Peck (1956), "Field Observations on Sand Drain Construction on Two Highway Projects in Illinois," Proceedings, Highway Research Board, Vol. 35, pp. 747-753.